ABSTRACT

WARM UNIT STAND ANALYSIS FOR PROTON IMPROVEMENT PROJECT II

Michael Pavlick, MS

Department of Mechanical Engineering

Northern Illinois University, 2022

Nicholas Pohlman, Director

The Proton Improvement Project II, commonly referred to as PIP II, is a linear accelerator overhaul at Fermilab to eventually double the output of its existing proton beam to continue to be the leading force in high energy physics. The proton beam is created through a series of high frequency cryomodules that must be connected utilizing a combination of magnets and vacuum pumps to ensure the beam is properly aligned. A housing mechanism for the magnets and vacuum pumps (Warm Units) will be placed between the cryomodules for realignment and require multiple stages of 6 degree-of-freedom adjustment options, to ensure that the beam alignment can fit all realistic requirements. Extensive testing and design modifications on the Warm Unit stand was completed to confirm not only the strength of the unit in nominal configuration, but also at each possible adjustment orientation for each 6 degree-of-

freedom option. Structural analysis was also completed for various unique loading conditions including transportation loading and confirming the unit satisfies international building code. Simultaneously, testing and design modifications were done to confirm that the frequency modes of the system resided outside of concern ranges, which is determined by Fermilab safety codes and is set to exceed 15 Hz. Design changes that simultaneously stiffen the system to raise the lowest frequency modes while expanding access for technicians and allow for easier fabrication were developed and implemented into the Warm Unit stand. Various relationships between the design changes and the overall vibrational patterns were also developed for future use and study as the rest of PIP II matures.

NORTHERN ILLINOIS UNIVERSITY

DE KALB, ILLINOIS

AUGUST 2022

WARM UNIT STAND ANALYSIS FOR PROTON IMPROVEMENT PROJECT II

BY

2022 MICHAEL PAVLICK

A THESIS SUBMITTED TO THE GRADUATE SCHOOL

IN PARTIAL FULFILLMENT OF THE REQUIREMENTS

FOR THE DEGREE

MASTER OF SCIENCE

DEPARTMENT OF MECHANICAL ENGINEERING

Thesis Director:

Nicholas Pohlman

ACKNOWLEDGEMENTS

Many were instrumental to the completion of this project. At Fermilab, this would not be possible without the help of Curtis Baffes, Kyle Kendrioza, Michael Geelhoeld and Joe Beleski. All their input and assistance were critical to the completion of the project, and without their guidance and expertise, the project could not be done. A special thank you is also due to Chris Becker for his magnificent work to get this project off the ground and set an excellent foundation. Also, to Nicholas Pohlman for his continued support and expertise and the opportunity to work on a project so interesting.

Contents

Definitions

FESHM- Fermilab Environment and Safety Hazards Manual

DOF- Degrees of Freedom

ANSYS- Finite element software

NX- 3D modeling software

Cryomodule- Main instrumentation for proton beam made of radio frequency cavities that are supercooled to 2K

Beam direction- The direction of travel between cryomodules, left to right when viewing the Warm Unit in a front view

Transverse direction- Perpendicular to the beam and gravitational direction

Vertical direction- Parallel to the gravitational force

PDR- Preliminary Design Review

FDR- Final Design Review

Chapter 1: Introduction

1.1 Background

For decades, Fermilab has been at the forefront of scientific discovery, mostly due to large-scale particle accelerator located in Batavia, Illinois. As the understanding of various proton related phenomena continues to evolve, a larger proton beam is required to keep up not only with the scientific demand, but also with the advancements of other countries. The Proton Improvement Project II (PIP-II) is the project that will bring Fermilab back to the front of particle research by replacing the existing linear accelerator (Lebedev, 2015). Table 1 below highlights the upgrades from PIP to PIP-II. The biggest upgrade, besides for doubling the beam energy, is the new dynamic nature of the system. As currently constructed, the proton beam is rigid and has limited capabilities for various cycles and intensity levels. With the upgraded PIP-II system, not only can experiments with greater beam energy be conducted, but a lot more flexibility in the type of experiment is possible.

Table 1: Upgrades for PIP-II'

Performance Parameter	PIP	PIP-II	Unit
Linac Beam Energy	400	800	MeV
Linac Beam Current (chopped)	25	2	mA
Linac Pulse Length	0.03	0.54	ms
Linac Pulse Repetition Rate	15	20	Hz
Linac Upgrade Potential	N/A	CW	
Booster Protons per Pulse (extracted)	4.2	6.5	10^{12}
Booster Pulse Repetition Rate	15	20	Hz
Booster Beam Power @ 8 GeV	80	166	kW
8 GeV Beam Power to LBNF	N/A	83-142*	kW
Beam Power to 8 GeV Program	30	83-24*	kW
Main Injector Protons per Pulse (extracted)	4.9	7.5	10^{13}
Main Injector Cycle Time @ 120 GeV	1.33	1.2	sec
Main Injector Cycle Time @ 60 GeV	N/A	0.7	sec
Beam Power @ 60 GeV	N/A	1	MW
Beam Power @ 120 GeV	0.7	>1	MW
Upgrade Potential @ 80-120 GeV	N/A	2.4	MW
* the first number refers to Main Injector operations at 120 GeV, second number to 60 GeV			

The proton beam is composed of a succession of different intensity cryomodules and their related instrumentation packages. The cryomodules, best visualized like a series of train cars in a line, contain super-cooled radio frequency cavities that allow for the proton beam to accelerate. Between each cryomodules is the instrumentation package, which can be a combination of different magnets, vacuum pumps, sensors, and anything else required to either continue the beam acceleration or measure and observe the beam. The cryomodules, shown in figure 1, and instrumentation packages vary throughout the beam length, however this project is in relation to the HB-650 MHz (high-beta 650 MHz) cryomodules, and its respective instrumentation.

Figure 1: Detail Model of Cryomodule

In between the succession of cryomodules (23 cryomodules will comprise the entire proton beam length), all "warm" instrumentation will be placed. The distinction of "warm" signifies that the unit is outside of the cryomodule, or in the room temperature air when compared to the inside of the super-cooled cryomodule. As the proton beam travels through the succession of cryomodules, acceleration is lost, so instrumentation to correct the trajectory of the proton beam is required. The instrumentation package ensures that the proton beam is in vacuum and aimed properly into the next cryomodule. The science behind the instrumentation is outside of the

scope of this project; however the size and interface connections have been determined and will be required to be adhered to in the design of this project.

For the 650 MHz region, the focus of this project, the gap between the cryomodules is approximately 1.3 m. The top of the alignment platform, or the top of the stand, is to be 120 mm below beamline, but otherwise the height is unconstrained. The do-not-exceed sizing envelope is also show below in Figure 3 and acts as the guiding principle for the sizing of the Warm Unit stand.

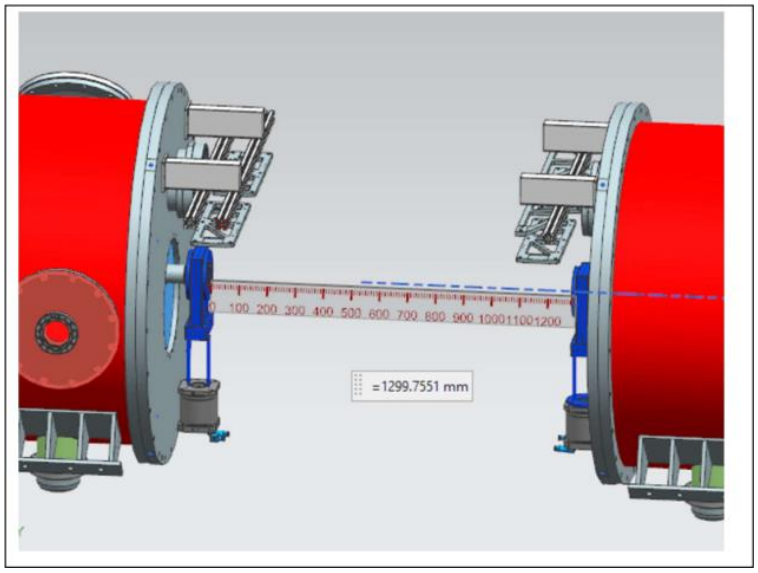

Figure 2: Gap Between Cryomodules, Where the Warm Unit stand Will Reside

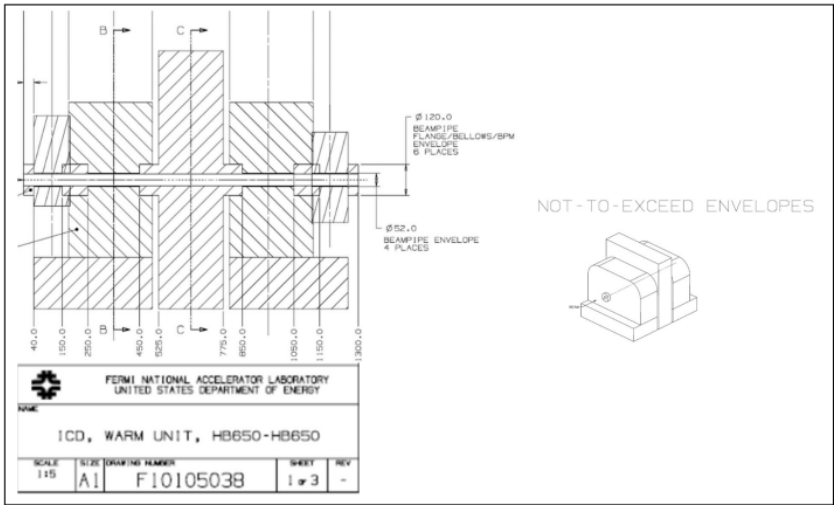

Figure 3: Dimensions of do-not-exceed envelopes in F10105038 of the interface control document

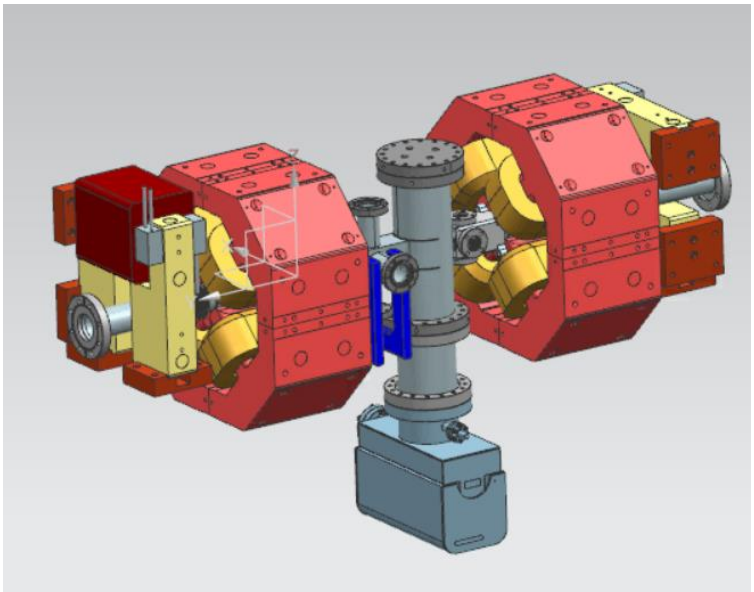

Figure 4: Instrumentation Package with instrumentation in grey with example quadrupole and dipole magnets in red and yellow 3D models

The instrumentation package, otherwise referred to as the payload of the system, is shown in figure 4 above. The entire single quad corrector package, the large red portion, weighs 350kg, the far outside of the package is the single direction corrector magnets and weighs 65 kg, and the inside portion, the vacuum pump, is projected to weigh 100 kg. All the designs from other

groups are dynamic and are expected to change slightly as the other design groups continue to mature their designs. However, a rough template for the overall size and mass of the instrumentation package has been unchanged and other design teams will be required to stay within the specifications the Warm Unit group has.

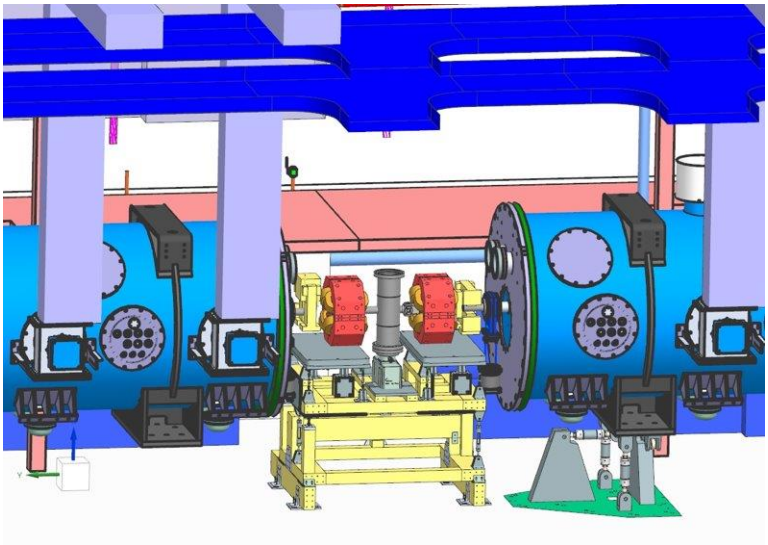

Figure 5: Warm Unit Stand in Relation to Cryomodules

Figure 5 above illustrates the Warm Unit stand within the size constraints of the cryomodules upstream and downstream. The Warm Unit stand is also shown holding the instrumentation package at the proper beamline height. The end deliverable of this particular project is illustrated in figure 5.

1.2 Design Requirements

The Warm Unit stand has quite a few design requirements to ensure that the unit can properly integrate into the PIP-II upgrade. The Warm Unit stand is to have multiple stages of 6 DOF adjustment, on both levels of the unit. 6 DOF means movement in all three directions, but also the ability for manipulation in pitch, yaw and roll for the entire unit, and just the individual portions of the instrumentation package as well.

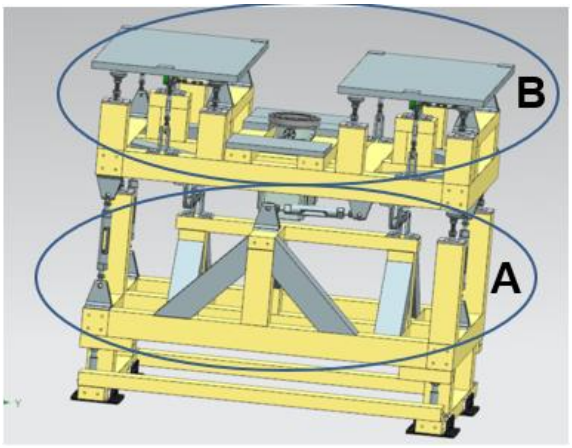

Figure 6: Course and Fine Adjustment Levels from PDR Design

The coarse stage, (A) in the figure 6, will have adjustability of +/- 30 mm in each direction, and the fine adjustment stages (B) have +/- 15mm local adjustment. The fine adjustment stage is where the actual instrumentation is supported, whereas the coarse adjustment stage is supporting the dual fine adjustment stages. The unit is to have full support from the floor to the beamline and have access to the instrumentation package from both sides of the unit.

The Warm Unit will also be primarily comprised of 8020 aluminum extrusion, apart from custom-made bracketing and plating, and custom-made turnbuckles that connect the levels of the Warm Unit stand and are the source of adjustability.

Another large design constraint is ensuring the repeatability of fabrication and ease of manipulation by field technicians. Between prototyping and actual installation, more than thirty

units will be created, so a focus on making the building process as simple as possible is critical. Once the unit is installed, a focus on making access to instrumentation and turnbuckle adjusters as easy as possible is also a design requirement. Finally, the turnbuckle adjusters are to be directionally independent. Meaning that manipulating one turnbuckle will have minimal impact on the adjustment of other elements in the kinematically determinant structure.

The final design constraint is integrating the Warm Unit stand into the surrounding infrastructure. The Warm Unit stand is to be installed with the surrounding cryomodules already in place, and limited spacing is available for bringing the Warm Unit stand into it's final positioning. Below illustrates the constraints, in particular in the beam length direction, that the Warm Unit stand must adhere to. Also, the Warm Unit stand will be subjected to a wide variety of low frequency, high amplitude vibrations through the concrete pad that the unit is anchored to. These frequencies are a product of surrounding infrastructure, in particular the surrounding pumps.

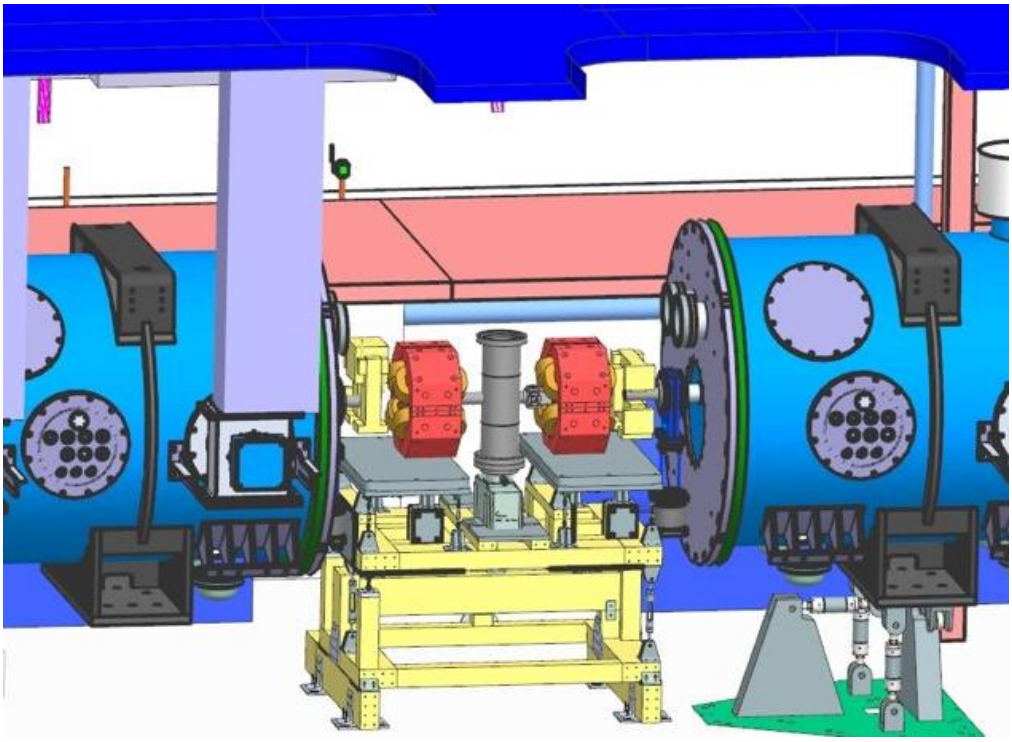

Figure 7: Warm Unit Stand Integrated Between Cryomodules

1.3 Previous Work

Previous work was done by Chris Becker (Becker, 2021) on the initial design of the Warm Unit stand in preparation for the Fermilab preliminary design review process. The design that Chris created captured all the requirements and was the general framework for the final design that was completed in this thesis.

The first, and most critical, component of the initial design created by Chris was the framework for a system that supported the structure from the floor to the beamline with the dynamic adjustability when under loading. The overall turnbuckle reliant design with the system of cascading rafts was maintained throughout the final design process.

Work done for the PDR also created a system for estimating the maximum local loading conditions as a function of individual rod length. Because the Warm Unit stand has adjustability

of +/- 30 mm in the coarse adjustment stage, and +/- 15 mm in the fine adjustment stage, the Warm Unit stand can be greatly manipulated if the extrema of the adjustment range are utilized. For example, if the left side turnbuckles are retracted completely, and the right side are extended fully, the coarse adjustment stage will twist the entire upper raft 30 mm over the 1.3 m length of the Warm Unit stand. Because of this phenomenon, Chris created a system utilizing factorial design to determine the worst possible loading conditions when the extrema of the rod lengths are implemented. “Factorial design is a process that narrows down all possible factors based on the maximum or minimum value of each variable in the experiment.” (Becker, 2021). This laid the foundation for all worst-case scenario testing to be completed later. The PDR level analysis also featured preliminary analysis of vibration modes of the simplified structure.

It was determined that before analysis was to be completed on the PDR level design, the representative stiffness is so be updated to more accurately represent the stiffness of the turnbuckles. This will not only directly impact the structural analysis of the system and the mass distribution, but the vibration patterns and the modal analysis required to satisfy implementation requirements. An updated floor mount design that can allow for field technicians to slide the unit into place while assembled and overall simplification to remove design reduandcy and technican accessibility are also major elements that require adjustment between the PDR and FDR stage of design for the Warm Unit stand.

1.4 Purpose of the Project

The intent of this project is to implement design changes to the PDR version of the Warm Unit stand, then do rigorous analysis and design change based off modal and structural analysis of the Warm Unit system. The initial pre-analysis design changes are the product of design review from Fermilab engineers. The pre-analysis changes were mostly improving access to the inside of the Warm Unit stand for technicians, removing redundancy in design and focusing on making the Warm Unit stand easy to manufacture on a large scale. This also includes a change to the floor mounting procedure, another effort to simplify fabrication and implementation. Once the initial pre-analysis design changes are implemented, modal analysis testing on the unit to confirm it meets all Fermilab vibration best practice requirements. Design changes that help move the natural frequencies out of the concern ranges and shape the vibrational behavior of the system will follow the pre-analysis changes. Once the unit is updated and modal analysis is confirmed to meet all requirements, extensive testing on the unit from a structural standpoint is to be completed. Once the unit is evaluated and updated to meet all structural requirements, a final test on the unit to confirm both modal analysis and structural analysis meet all requirements and the unit is as simple and resource efficient as possible will be performed. Upon completion of all testing, an eventual prototyping phase will begin, but that is outside of the scope of this project.

1.5 Updated Design

A Preliminary Design of Warm Unit Structures was performed in 2021. Since that time, to make the Warm Unit stand simpler for production and easier for field technicians to work on, simplifications to the overall design were implemented to streamline the unit while maintaining the strength and overall dynamic flexibility of the system. The main structural features and dynamic nature was maintained, though an emphasis on simplifying assembly and allowing for greater ease of operation and access slightly changed the design. One of the largest changes was the removal of vertical supports in favor or plating, as shown in figure 8.

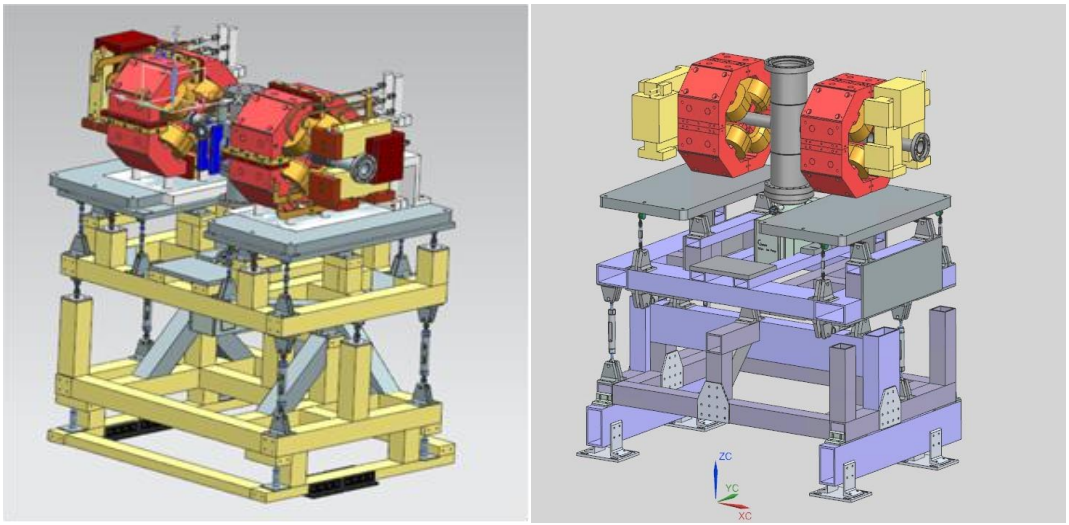

Figure 8: PDR Stand with 45-degree Grey Supports(left), Model of FDR Warm Unit Stand Utilizing Plating(right)

As shown above, stiffening plates added to the center section improves access to the inside of the section. The bottom portion, or the floor connection, was also updated for implementation and ease of fabrication. Figure 8 also highlights the updated floor connection. The yellow representation(left) highlights the previous design that limits the floor access and ability for simple transportation. An updated design, shown in purple on the right, creates greater access under the unit while simplifying transportation.

Other small design features were implemented before modal analysis was completed on the updated design:

- Removal of redundant components
- Expanding the wheelbase(i.e. transverse separation of vertical supports) to reduce load distributions
- Adjusting the turnbuckle height

The floor connection also underwent significant development. In favor of simplicity and ease of repetition, the floor raft was replaced with guiding rails placed between the cryomodules, as shown below in figure 9.

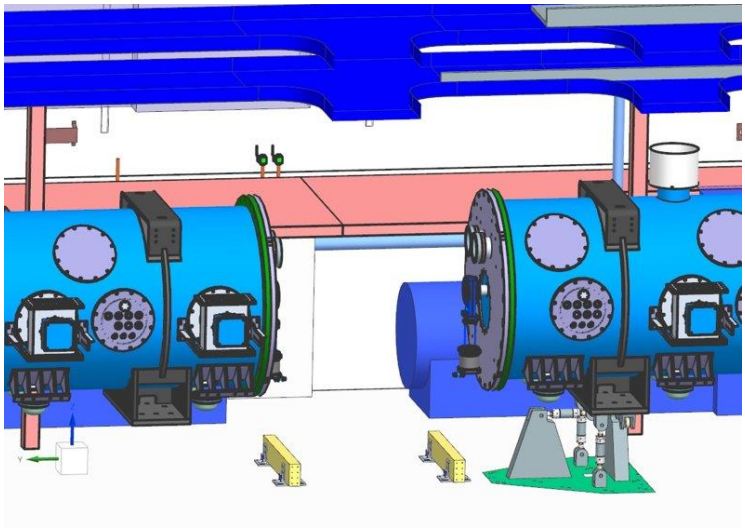

Figure 9: Bottom Floor Connections or the Guiding Rails

Floor mounts are shimmed to offset imperfections in the floor, shown below in figure 10. Once the floor mounts are confirmed to be perfectly in line and level utilizing the shim pack, the mounts are secured to the floor utilizing anchor bolts into the cement floor.

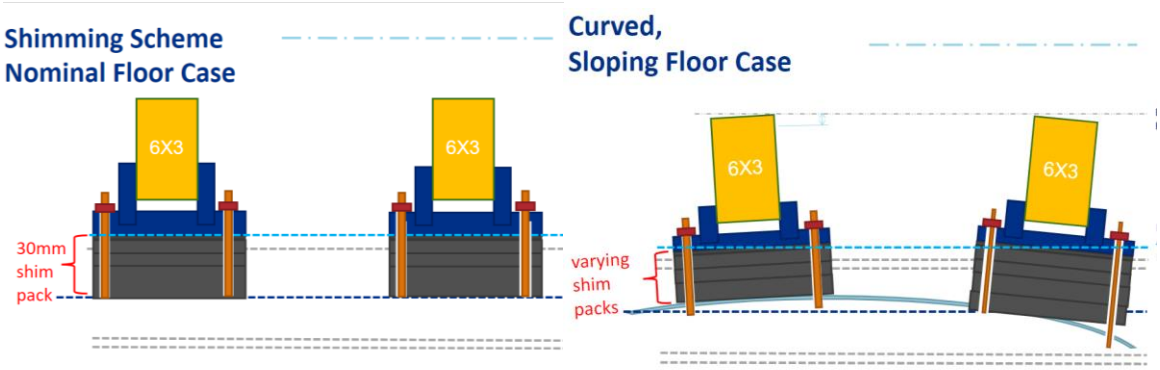

Figure 10: Nominal Shim Stack (Left) and Curved Floor Stack Example(Right)

Figure 10 above shows how the shim pack can be changed to ensure that the guiding rails are properly aligned for the rest of the unit to be placed on top. Due to the simplicity of the new floor mounting system, by just adjusting the height of the shim pack the guiding rails can be brought to the same height.

Once the guiding rails are added, the rest of the Warm Unit stand is slid into position and secured utilizing not only the weight of the system, but bracketing between the unit and the guiding rails, shown below. The Warm Unit stand and the connecting rails will make contact utilizing ¼" steel shims directly in line with the vertical load lines, shown below. By only having contact at these three particular spots, the risk of tolerance stacking due to imperfections in the 8020 material is mitigated. For example, if the guiding rail was slightly misaligned and the 8020, while still within specifications, was not entirely straight and the pieces were fastened together, it would create uneven loading on the fasteners or possibly create added instability if the connection does not span the entire length of the 8020.

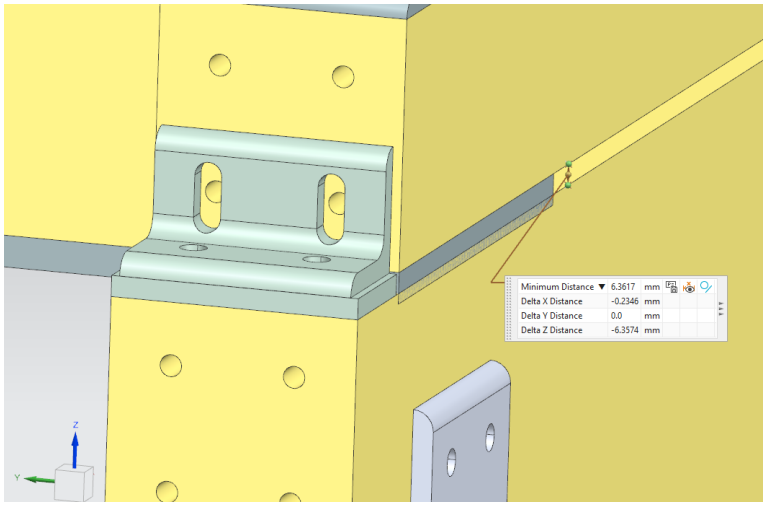

Figure 11: 1/4" Shim Between Guiding Rails and Warm Unit stand

Figure 11 shows how simple 90-degree bracketing will sufficiently hold the unit in place during use after the unit is placed onto the guiding rails.

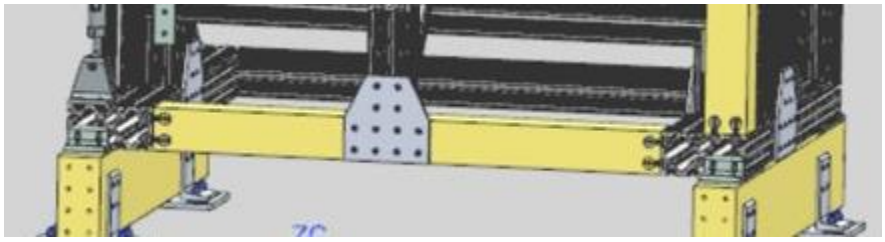

Figure 12: Coarse Adjust Stage Connection to Rails

After the Warm Unit stand is connected to the guiding rails, the rails slide into place on the floor mounts, shown in figure 13 below. Between the guiding rails and the floor mounts, a bearing bronze plate will act as a low friction sliding solution so the entire unit can slide into place on the floor mounts.

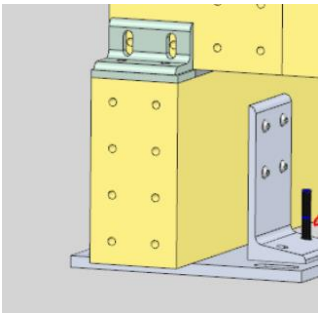

Figure 13: Glacier Plate Location

Though technically the initial design changes are not due to the structural and modal analysis, the flexibility in foundation will drive the weight distribution for structural analysis and the overall stiffness, in the transverse direction particularly, for the vibrational patterns of the system. This will act as the framework for the rest of the analysis completed.

Chapter 2: Simulation Parameters and Performance Requirements

2.1 Simulation Parameters

To make the simulation possible and a proper precursor to an eventual prototype testing, analysis is completed in ANSYS (ANSYS, Inc. , R2020). Though the goal is to properly replicate the final model as closely as possible, slight alterations with minimal impact on the overall accuracy will need to be taken into consideration for analysis to be time and resource effective.

The first simulation change is the replacement of the turnbuckles with the spring feature in ANSYS. It is important that the springs are used because they simplify recovery of loads at each strut in this statically determinate system and are also more computationally efficient than fully meshed struts which have already been analyzed as a standalone feature (Becker, 2021). By reverse engineering the stiffness of the springs from turnbuckle analysis previously done, the system can be simplified while maintaining the exact same structural and functional integrity of using the springs. Previous analysis greatly overestimated the stiffness of the springs, where the stiffness done in this analysis is modeled at 1.25 x 10^8 n/M. This stiffness was derived by taking the force applied to a fully assembled turnbuckle and determining the overall deformation or elongation of the turnbuckle, then simply using the same rate of deformation for the spring.

Another ANSYS feature to be considered is the actual geometry of the 8020 material itself. The vast majority of the Warm Unit stand is comprised of various pieces of 8020 aluminum extrusion for its ease of use as a variable length dimension, joints that produce square corners, and effectiveness in fabrication and cost. The 8020-extrusion geometry is shown in Figure 14 has 3 main features: 1. A central square that is open in the center to reduce material and weight; 2. Slots in which nuts can be placed for locating position anywhere along the length, and 3. Corners that maintain the square external dimension for sizing structures (8020 I. , 2022). The complex cross section would require significant meshing by ANSYS increasing

computational time even though the loading structure is carried by the central core like a beam. A simplified version of the geometry was created to replicate the physical properties (specifically bending stiffness) of the extrusion while allowing for simulation software to mesh and interact with the material. The representative 8020 captures bending stiffness accurately, while only capturing 75% of the actual axial stress. Calculations of the moment of inertia required to calculate the bending and torsion stresses are shown below, where the moment of inertia of the more complicated 8020 extrusion is captured utilizing a simplified rectangular extrusion. By accurately maintaining the moment of inertia, the bending and torsion is representative of the true behavior from the 8020 extrusions. However, with the updated geometry, the cross-sectional area is reduced. For axial stress, which is simply the relationship between the applied force and the geometry, the axial stresses will be overestimated due to the reduced area. This builds in a small buffer and allows for a small factor of safety to be built into analysis for axial stresses, while accurately representing the torsion and bending stresses. A cross sectional view of the simplified geometry is show below in figure 14.

$$142.07\ cm^4 = \frac{(7.62cm)^4 - b^4}{12}$$
$$b^4 = 3371.48cm^4 - 1704.87cm^4$$
$$b = 6.39cm$$

- Cross-section of 8020 3030 section (left)
- Aluminum tube for future analysis (middle)

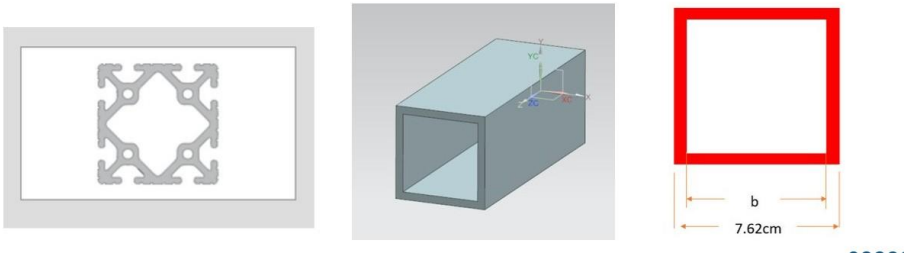

Figure 14: Cross Sectional 8020 View and Moment of Inertia Conversion

The new representative piece of 8020 conservatively represents the directional strength of real 8020 while maintaining simplicity for cross sectional geometry. The axial strength is

approximately 75% of a true 8020 section, building in an extra level of conservation in assumptions.

In similar fashion, the payload geometry is composed of multiple components too complicated and requires far too many resources to properly model in ANSYS. Pseudo masses that exceed the production expectation by 10% for the magnets and overestimate the center vacuum pump instrumentation section by close to 50% were created to accurately represent not only the mass of the eventual instrumentation package, but also for the center of gravity and associated moment of inertia associated with the complicated geometry of the instrumentation package. This also allows for flexibility later in the process as the instrumentation package becomes closer to finalized, the pseudo masses can be easily adjusted to make slight changes to accurately reflect the final design of the instrumentation package.

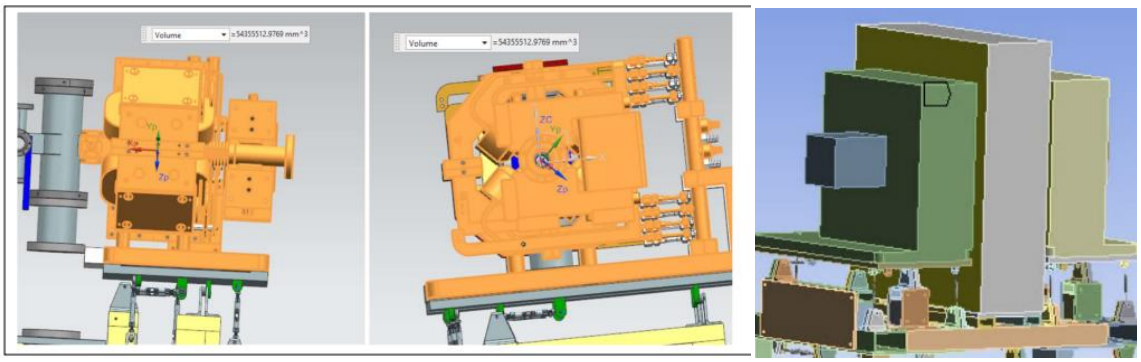

Figure 15: Corrector Magnets (Left) and Pseudo Mass Replacements (Right)

The floor connection was also slightly simplified. In use, the floor mounts will be mounted with a combination of shims being anchored using floor anchors and bolts. This connection was simplified by just securing the base plates directly to a fixed plane that functioned as the floor.

2.2 Simulation Simplifications

One small simplification that was required was bonding 8020 pieces together that did not share an adequate amount of cross-sectional area. Due to the simplified representative geometry, the connection between pieces of 8020 that required direct use of the interface shown in figures 16 and 17 below to connect with another section of 8020 did not represent the proper joint between the two through standard fasteners. By manually bonding the pieces together, utilizing the bonded contact feature in ANSYS, it more accurately represents the connection between two 8020 pieces with complex cross-sectional geometry.

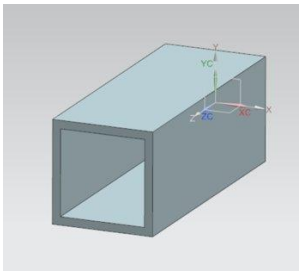

Figure 16: Cross Section of Representative 8020 Section

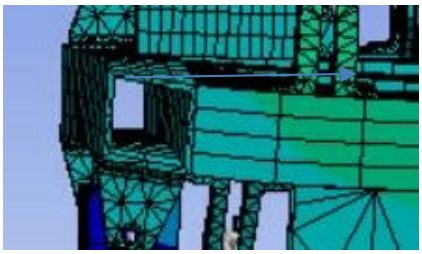

Figure 17: 8020 Connection Deformation

Figure 17 illustrates the exaggerated movement, shown by the 8020 separating, due to the lack of material interfacing. The bonding more accurately locks the sections in together to mimic the actual connection. It was found that the greatest horizontal loading is under 2 KN, and double 8020 fasteners can withstand a direct load of 2000 lbs., so no separation will occur.

The top raft of the Warm Unit stand also required a slight simplification. For the vertical connection between the coarse and fine stand, or the middle and the top of the warm stand, three turnbuckles are utilized. Support pieces are located opposite to each turnbuckle for added vertical support, shown below in figure 18. They are vertically oriented pieces of 8020 with an adjustable leveling jack that is extended to meet the upper raft once turnbuckles are installed.

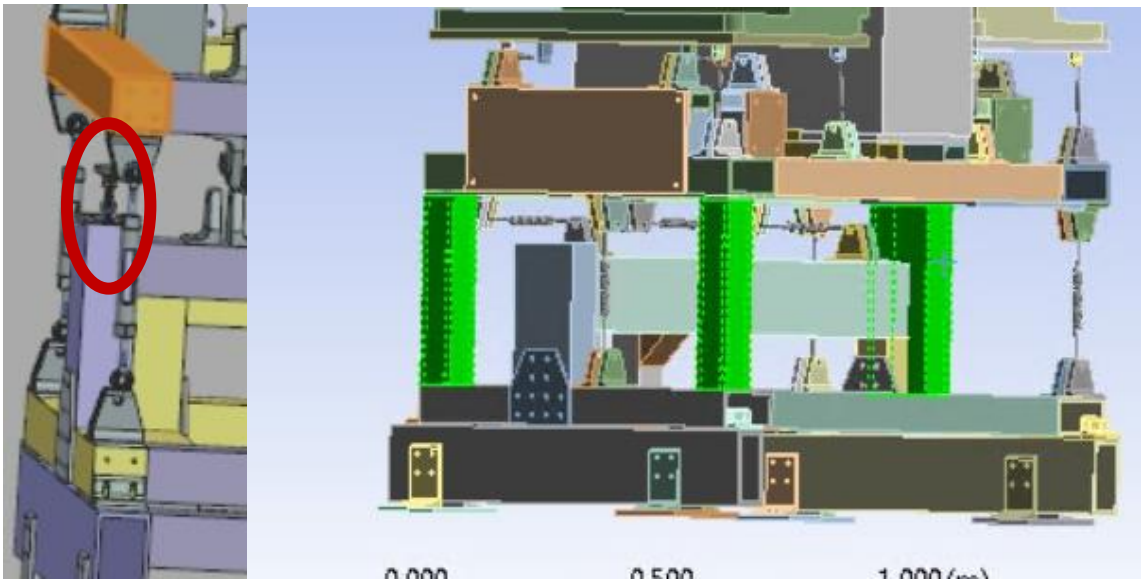

Figure 18: Vertical Support Replacements

For simplicity, the leveling jacks are replaced with 8020 shims, shown above. The leveling jacks are significantly stronger than 8020 in a vertical compressive orientation, meaning that the shim replacement maintains the conservative nature of the simulation to prevent moving in gravitational direction but allow translation on the plane of the connection. In reality, the friction forces between the feet material and the 8020 structure will provide dampening which would affect the real-world frequencies in modal testing.

.

2.3 Modal Analysis Requirements and Set-Up

The Warm Unit stand is required to have its lowest natural frequencies > 10Hz (Baffes). Because of the difficulty of faithfully capturing all relevant details of a real system (e.g., joint compliance) in modal analysis, the team adopted a self-imposed goal of >15Hz for the lowest modes of the system.

2.3.1 Constraints

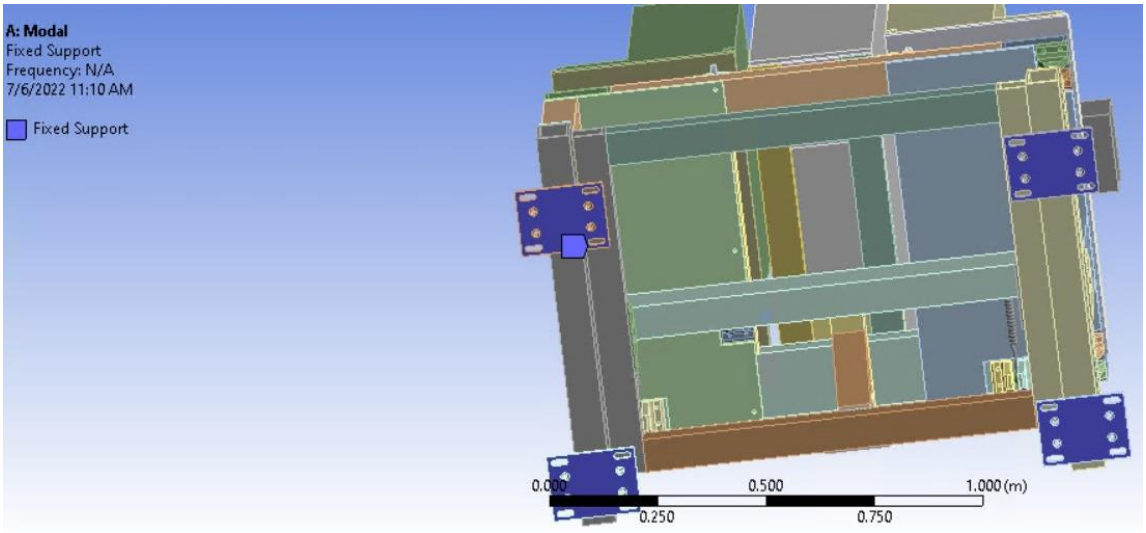

Figure 19: Floor Constraints on Warm Unit Stand

The floor connection is quite simple. Because the floor mounts will be sitting on a stack of shims, it can be assumed that the mass will be distributed throughout the entire floor mount. With that assumption, the entire floor mount base can just be fixed to the floor without sacrificing any accuracy while making the simulation more efficient.

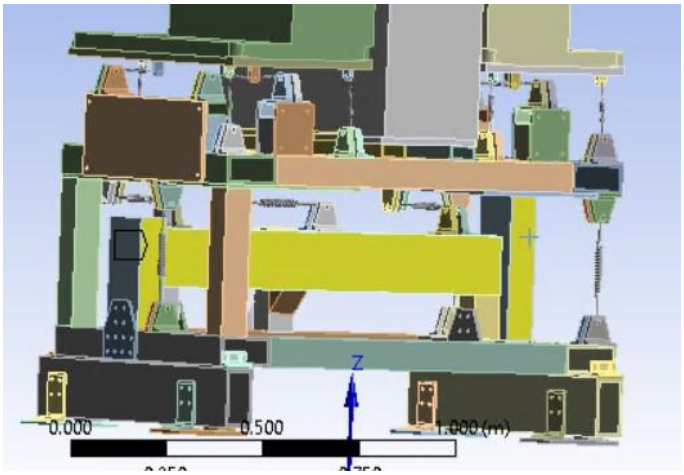

Figure 20: Coarse Adjustment Spanner Connection

One of the few constraints with the actual unit was bonding the yellow highlighted sections of 8020 shown in figure 20 together. Because the representative geometry has a small connection area compared to an actual piece of 8020, a constraint to keep the pieces tied together was added to the modal testing. This is a fair constraint to place, as the system is under minimal transverse loading, as seen in structural testing. A similar bonded constraint is applied to the angle brackets that hold the Warm Unit stand to the guiding rails.

2.3.2 Loads

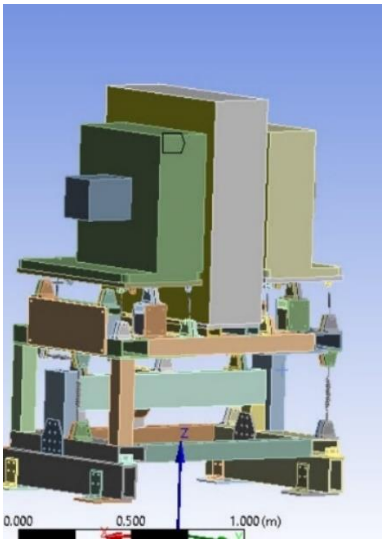

Figure 21: Loading Conditions for Modal and Structural Analysis

The loading for the modal analysis is also extremely simple. The pseudo masses capture the weight and center of gravity of the payload, so the masses of the pseudo masses are the only loading in the nominal configuration modal analysis testing. Table 2 shows the pseudo mass sizes, and the corresponding center of gravity locations.

Table 2: Pseudo Mass Sizing and Center of Gravity Locations

Payload Replacement Pseudo Mass Size	**Beam direction(inches)**	**Transverse direction(inches)**	**Height(inches)**
Center vacuum pump	11.22	31.89	38.97
Quad magnet	9.85	23.51	24.01
Corrector package	9.04	7.16	7.16
Center of Gravity			
Orientation: Vertical is distance from top of reciever plate, beam direction is distance from center of warm unit and transverse is distance from aisle side edge			
Center vacuum pump	5.61	15.945	19.485
Quad magnet	4.925	11.755	12
Corrector package	4.52	3.58	3.58

2.3.3 Connections

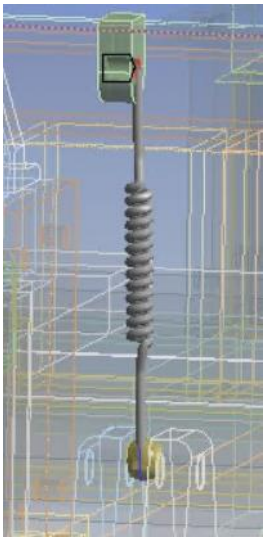

Figure 22: Turnbuckle Connection

Figure 22 shows how the spring is connected at both ends. A ball that represents the rod end is added between the two brackets. The ball that replaces the turnbuckle rod ends are needed to ensure that the shear stress is distributed between the two brackets evenly and the stress more accurately reflects a real application of the turnbuckle. On the other end, the spring is just directly connected to the end of the connection hole in the tabs. Shown below in figure 23 is a closer view on how these are connected. It should be noted that due to the angle it looks like the tab connection has the spring going through the tab, though it is slightly outside of the tab.

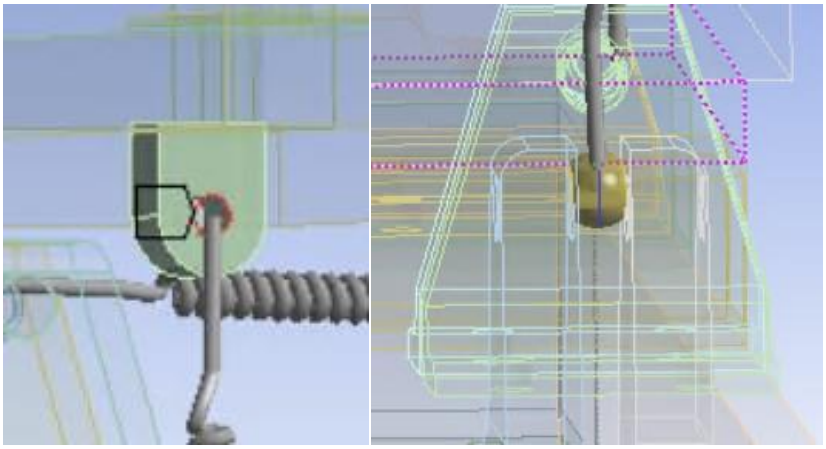

Figure 23: Ends of Turnbuckle Springs

2.3.4 Meshing

For modal analysis, a simple swept mesh was utilized. For some of the larger components, the pseudo masses in particular, the mesh is unimportant. The bracketing required a smaller (.002 m) element size when compared to the rest of the system, just for a greater understanding of the stress and deformation pattern. The element sizing on the 8020 pieces was also changed to a smaller (.02 m) size, partially for greater accuracy but more important so the unit will have multiple nodes in each direction. Simple ANSYS meshing did not have multiple nodes in each direction, so sizing was required (ANSYS, 2022). Figure 24 below shows the meshing of the entire system in modal configuration.

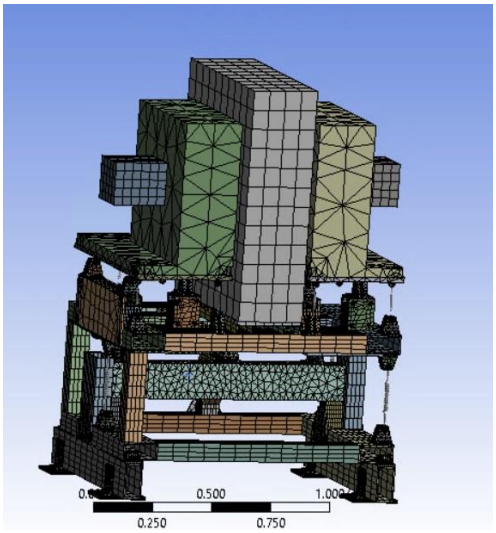

Figure 24: Warm Unit Stand Meshing

2.4 Structural Analysis Requirements and Set-Up

2.4.1 8020 Aluminum

8020 aluminum extrusion is a "modular T-slot aluminum building system for every industry or application" (8020 I. , 2022) that is incredibly useful for applications similar to the Warm Unit stand. 8020 is best envisioned like a more dynamic version of LEGOs, that allows for great adjustability. The 8020 extrusion is allows for sliding along the axial direction for objects such as bracketing or plating and offers a wide variety of connections in all possible orientations. 8020 is also an advantageous piece to work with due to the weight to strength ratio, the tight tolerances to ensure straightness, and unit components can be directly assembled by 8020 vendors.

Though 8020 aluminum is relatively strong, it is important to ensure that the unit is not under a concentrated load large enough to deform the material. According to FESHM Chapter 5100: Structural Safety (FERMILAB), the load stress should not exceed 60% of the maximum yield strength. According to the 8020 distributors, the yield strength of 8020 aluminum extrusion is 35,000 PSI, or approximately 241 MPa. Because simulations are using a representative piece of 8020 and adaptability to be able to eventually add more instrumentation if needed that would increase the size of the payload is preferred, it is critical to not come close to any of the maximum values. It will also be seen in later analysis that under unique loading, worst case loading for example, could concentrate loads and create areas of concern, so it is important that the unit does not come close to approaching 144.6 MPa in nominal configuration.

The entire unit was simply fixed to the floor utilizing the floor mounts. A fixed condition on the plates accurately represents how the unit will be connected to the floor in use. The pseudo masses of the system were changed to structural steel to accurately represent the weight and the CG of the actual payload. The center mass, or the vacuum pump package, was 100 kg. The

quadrupole magnets, directly to the left of the vacuum pump, is 350 kg, where the final corrector magnet was 65 kg, located at the positions previously shown in table 2.

For this simulation, a simple swept mesh was utilized. For some of the larger components, the pseudo masses in particular, the mesh is unimportant. The bracketing required a smaller (.002 m) element size when compared to the rest of the system, just for a greater understanding of the stress and deformation pattern. The element sizing on the 8020 pieces was also changed to a smaller (.02 m) size, partially for greater accuracy but more important so the unit will have multiple nodes in each direction. Simple ANSYS meshing did not have multiple nodes in each direction, so sizing was required.

2.4.2 Turnbuckle Analysis

Previous analysis completed for the PDR concluded that the large coarse adjustment turnbuckles, when made of 4340 steel, can withstand a 7000 N force safely (Becker, 2021). If required, the turnbuckles can be stiffened with a more expensive material, however in current configuration it is estimated that 7000 N is acceptable.

Using the same testing procedure of adjusting each length independently and then adding as super-position, Chris Becker determined that the maximum force was approximately 3000 N for smaller upper raft turnbuckles. The upper raft will not have the vertical loading, and require less adjustment, so it is understood that it does not require the same rigidity.

By reverse engineering the relationship between material stress and the deformation of the turnbuckles under testing, it was determined that the ultimate failure point is 23.6 KN and 25.2 KN for the large and small turnbuckles, respectively. The larger turnbuckle has a slightly lower maximum failure point because the added length to the turnbuckle shank, in particular on the corners of the wrench adjustment area, creates a greater bending moment force. This ultimate failure point was determined by finding the relationship between the force applied and the

concentrated stress on the turnbuckle material. Because any changing in area can reasonably be assumed to be negligible, by using the area of the turnbuckle and the maximum allowable stress for 4340 steel (60% of yield stress), a maximum force that corresponds with the material reaching the maximum allowable stress can be determined as the maximum allowable.

Spring probes were added at every turnbuckle connection to ensure not only that the turnbuckles will not be at risk of deformation or failure, but also that the unit is not unevenly distributed to a detrimental level. It is impossible, and simply not important enough, to get all the complimentary turnbuckles supporting the same amount of weight so everything is under equal loading, but the loading needs to be spread out to some degree so a single strut is not carrying an exceptionally large load. The best example of this is the three vertical struts in the coarse adjustment stage. The loads do not need to be identical, however one side cannot have over double the loading of the other.

2.4.3 Bracketing

During early testing, it was determined that in some worst-case scenario orientations, the size loading on the commercial-off-the-shelf (COTS) brackets (8020, 2022) could approach dangerous levels of deformation exceed 1.5 mm. Custom made brackets were made utilizing a standard L-bracket from McMaster-Carr, by machining the ends from the bottom and adding in the fixture holes. The updated design implements three main changes: the material, geometry, and the manufacturing process. The bracket was upgraded to 4340 steel to match the turnbuckle strength and the material thickness was increased in the direction of major displacement. Details of the new bracket design are shown in the modal analysis section, as the bracket update is a result of modal analysis testing.

From structural analysis testing, it was concluded that the maximum force on a vertical strut in nominal configuration was 1932 N, and negligible force in the horizontal direction for the

coarse adjustment struts. For the fine adjustment struts, the maximum vertical was 299 N and the beam direction maximum was 28.2 N. By making a test fixture, it can easily be determined if the brackets will be able to withstand the force. Like 8020, 60% of the yield strength is the maximum stress, or 280 MPa for 4340 steel. If the stress is low enough, 4340 steel will be used for cost and production efficiency.

2.4.4 Worst Case Scenario Loading Parameters

The adjustable nature of the Warm Unit stand and the isolation of each 6 DOF control (to first order approximation) is the unit's strong point, but it offers a challenge in ensuring that the unit will be safe to use under the extreme ranges of positions and rotations. Because the coarse stage can adjust up to 30 mm in each direction, and the fine adjustment stage 15 mm in each direction, if all the turnbuckles are at extreme lengths, meaning their lower or upper value, it can cause the pseudo masses to be manipulated in a way that could impact the performance through unique locations of the center of gravity relative to nominal set-up conditions.

The way that the worst-case scenario testing was completed was relatively simple. Previous analysis was done with each combination of rods either completely retracted or completely extended for the coarse and fine adjustment rafts, respectively, while assuming uniformly distributed loads (Becker, 2021). The loads on each turnbuckle were collected and the greatest force on one particular turnbuckle constituted a loading configuration as "worst case." The top few worst combinations for loading were taken from the initial testing on the old unit and were used directly on the updated design. For simplicity, instead of adjusting the individual rod lengths and the re-adding the springs, the rafts were just twisted in conjunction and the springs were connected to the new connection points. For example, one of the worst

combinations was when the vertical struts on the coarse adjustment were at extreme opposite lengths on opposite sides, meaning that the end with two vertical rods were all the way extended, whereas the single strut was retracted all the way, shown in figure 25 below.

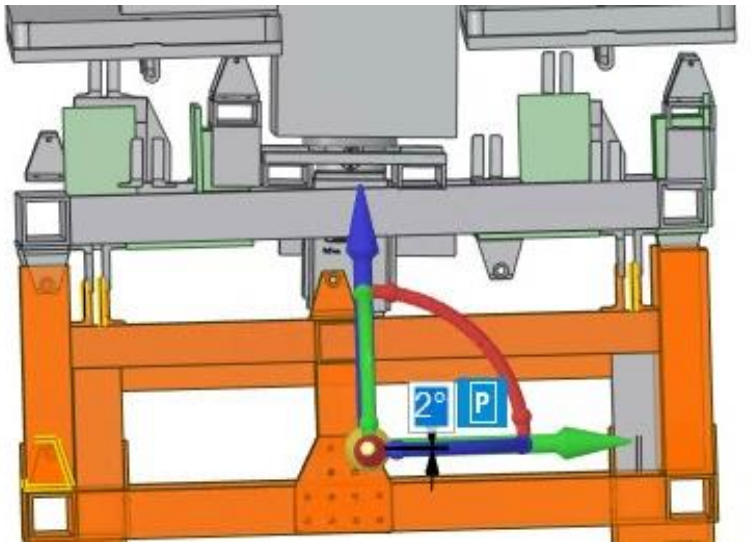

Figure 25: Coarse Adjustment Raft Being Manipulated for Worst Case Loading

This would slope the unit and force the mass of the system down on that edge of the raft, shown below in figure 25. The way that the angle was modeled was by reverse engineering the difference in strut lengths over the distance of the beam length width and determining the angle that the raft will sit at. With a maximum vertical displacement difference of 30 mm spanned over the 1.3 m raft, the angle at which the raft was twisted was 1.32 degrees. The same logic was applied to all other configurations. The transverse direction could move up to 2.1 degrees. On the upper raft, the vertical displacement was .65 degrees, and transverse 1.05 degrees.

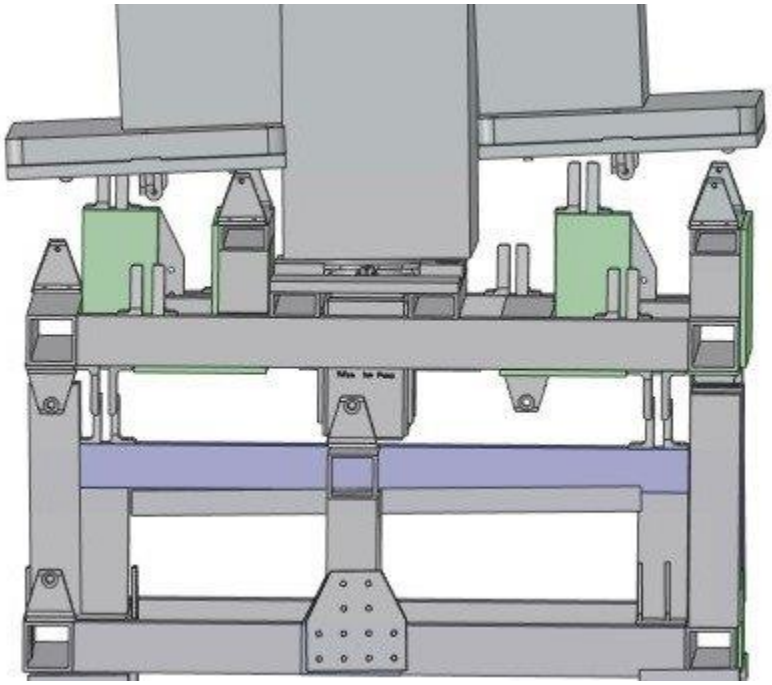

Figure 26: Worst Case Loading Example for Upper Raft

The worst loading cases were always when the masses were pointed down in the direction of corner of the unit. Though they have influence, it becomes evident that the transverse beam direction struts do not play a significant role in large deviation from the overall strength, because it is so vertically dominant.

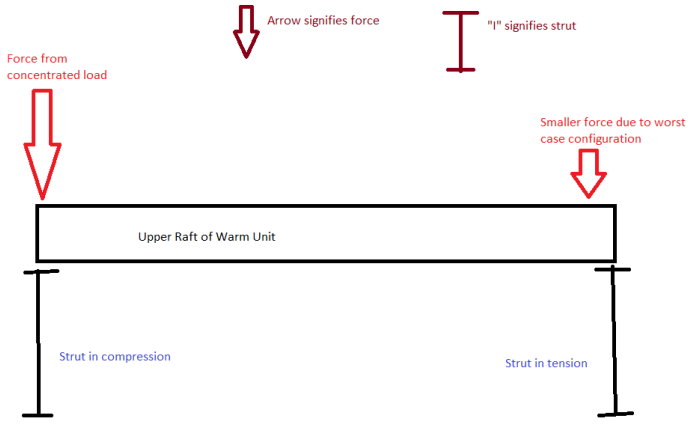

Figure 27: Upper Raft FBD Under Worst Case Loading Sketch

Figure 27 above illustrates how concentrating loading onto one side of the upper raft will place the opposite strut in tension.

Chapter 3: Modal Analysis of Warm Unit Stand

The initial design testing yielded the results shown in table 3 below. All six modes were below the required frequency.

Table 3: Initial Modes of Warm Unit Stand

Mode	Hz
1	0
2	0
3	0.6
4	2.3
5	3.7
6	5.22

Though as long as the entire design can be manipulated as long as the design changes meet all the requirements, some design changes minimize the impact on other components of the PIP-II project. The main few design changes, or adjustment knobs, that can be manipulated are adjusted throughout the modal analysis design section.

The strut locations and sizes can be manipulated to satisfy any design change or design feature deemed necessary. This can be not only the strength of the strut, or the corresponding bracket, but also the location of the struts in relation to the rest of the Warm Unit stand raft. As long as the turnbuckles do not interfere with 8020 connections of the instrumentation package and they maintain the one degree of freedom singularity, the location can be manipulated however it is deemed necessary.

In a similar respect, the sizing of the 8020 aluminum extrusion can also be manipulated to achieve any design change. The 8020 can also be manipulated using steel plating or gusset bracketing to achieve desired stiffness or connection strength.

In essence, as long as the design requirements are still met and the access to the implementation package isn't limited, anything can be changed to a certain extent.

3.1 Stiffness Through Design Change

The following tests are to create a greater understanding of the relationship between various design components and the overall modal behavior. All the mentioned testing contributed to the final design, as most were just directly implemented to the final unit.

3.1.1 Spring Stiffness

First a relationship between the turnbuckle replacements, or the spring stiffness, and the modal behavior was determined. The following shows the frequencies at each spring stiffness.

Table 4: Modes for 3000 N/m Spring Stiffness

Mode	Hz
1	0
2	0
3	0.6
4	2.3
5	3.7
6	5.22

Table 5: Modes for 3,000,000 N/m Spring Stiffness

Mode	Hz
1	0
2	1.97
3	4.9
4	5.3
5	8.4
6	11.6

Table 6: Modes for 3,000,000,000 N/m Spring Stiffness

Mode	Hz
1	0
2	2.12
3	6.92
4	9.85
5	14.57
6	17.49

Though the first mode does not change, it becomes apparent that at the greater stiffness, the later modes begin to raise. This suggests, as expected, that the Warm Unit stand vibrational stability is based largely on the vertical stiffness of the system.

3.1.2 Material Properties

After a relationship between the turnbuckle strength and the stiffness was determined, a relationship between the material properties and the modal behavior was determined. In an effort to understand if the unit was stiffer, all the material assignments were changed to stainless steel. It was found in other testing that upgrading the material from aluminum to stainless steel a decent representation of upgrading to the larger 8020 extrusion could be replicated without a full redesign.

Table 7: Modes for Aluminum Alloy

Mode	Frequency
1	3.696
2	4.343
3	6.061
4	6.6289
5	13.842
6	16.506

Table 8: Modes for Steel Alloy

Mode	Frequency
1	5.96
2	6.84
3	9.65
4	10.47
5	21.31
6	24.66

As shown above in tables 7 and 8, the system becomes stiffer with a greater material yield stress. This allows creates the rule of thumb that adding more material to high deformation areas or adding support plates would raise the frequency values.

3.1.3 Coarse Adjustment Analysis

Then testing on just the coarse adjustment was completed, to get the current main source of instability to a level of proper stiffness. It became clear that the greatest deformation was in the coarse adjustment stage, so focusing on stiffening that portion became the priority.

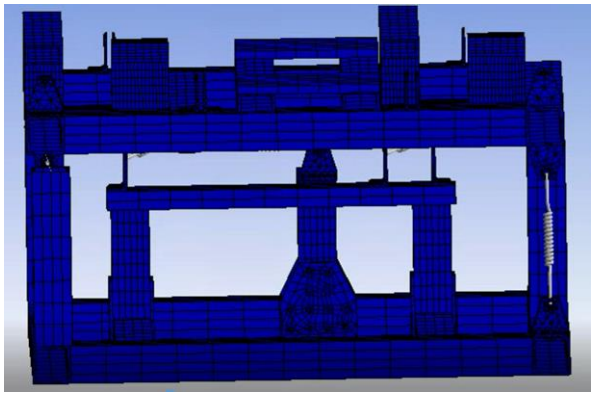

Figure 28: Coarse Adjustment Stage

The next testing was to determine if the instability in the coarse adjustment stage was due to vertical displacement from the top raft, or displacement in the beam direction (left to right).

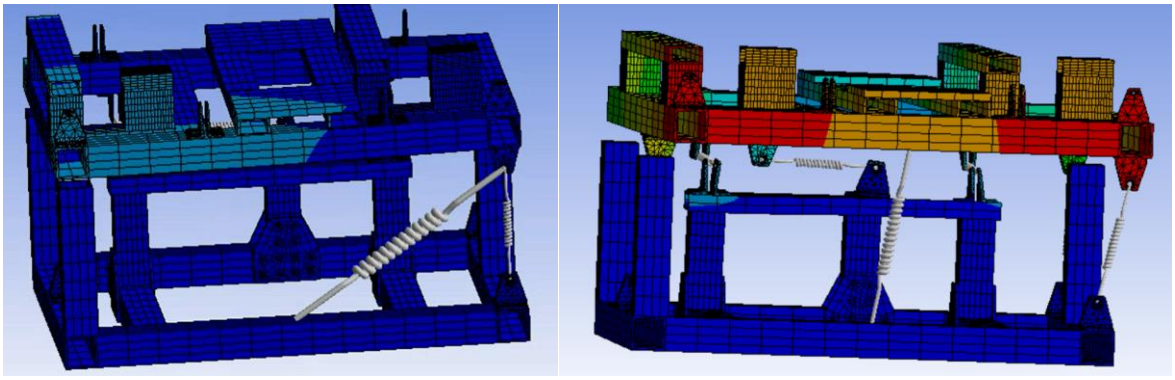

Figure 29: Stiffening Spring Orientations for Vertical and Beam Direction Displacement

By adding a stiffening spring in two different orientations, shown above, it was determined that greater stiffness is achieved by limiting movement in the beam direction, shown in figure 29 on the left, more than vertical displacement.

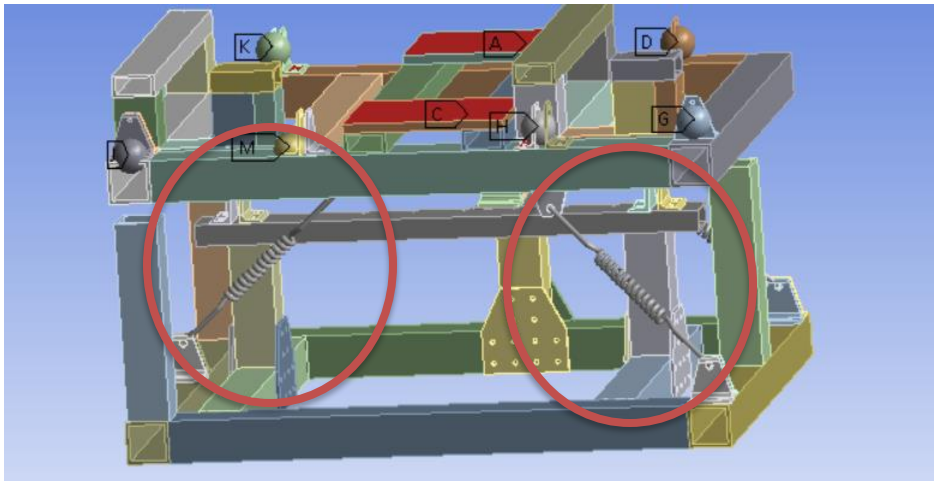

Figure 30: Transverse Direction Spring Stiffness Added

Next, testing on the transverse direction (highlighted above in figure 30) by locking the highlighted areas in place raised the lowest frequency to over 25 Hz. It became clear that this portion of the coarse adjustment deforms too easily and needs to be stiffened. The fixed constraints are obviously not permanent but help get a better understanding of where instability is derived.

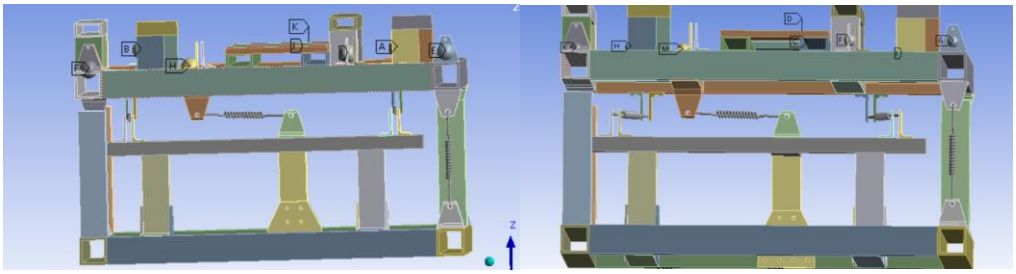

Figure 31: Extending Transverse Struts Outwards

From this point, the locked portion was unlocked and then the wheelbase of the innter connection was extended, shown in figure 31. The transverse struts were moved towards the edge of the raft 50 mm at a time, until they reached the end. It was determined that by moving the transverse turnbuckles outward and tie them into the sides of the unit, more stiffness can be derived, as shown below.

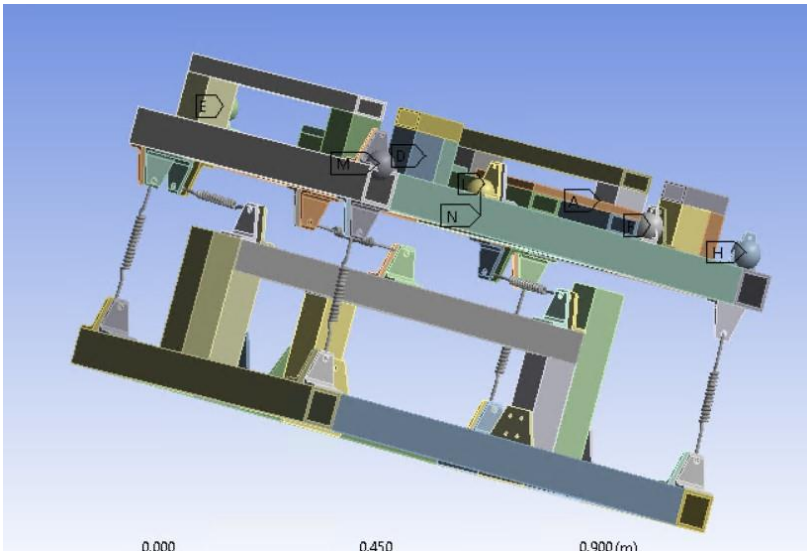

Figure 32: Upgraded 8020 Extrusion to 3030 Option

The 8020 that hold the transverse struts was also upgraded to the larger 3030 extrusion for extra stiffness, also shown in figure 32. By moving the wheelbase out to tie into the outside of the raft and by upgrading the material to a larger extrusion, the overall stiffness grew.

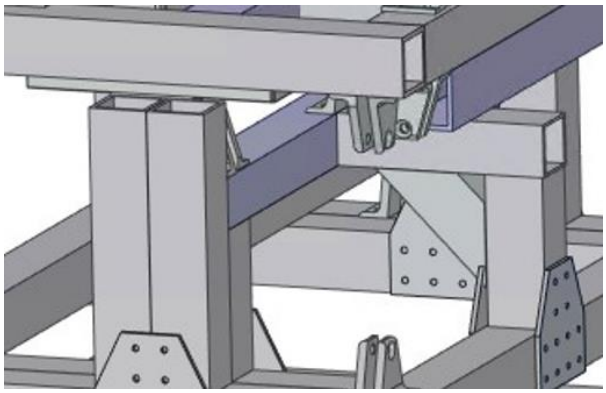

Figure 33: More 8020 Added to Coarse Adjustment Stage

More 8020 was added to the vertical supports, a spanning piece under the beam direction 8020 and a 45-degree angled piece were all added for the same reasons. Reconfiguring the center of the coarse adjustment stage grew the stiffness, shown in table 9 below.

Table 9: Coarse Adjustment Stage Modes

Mode	Freq(Hz)
1	11.021
2	20.73
3	22.02
4	33.61
5	53.75
6	64.05

3.1.4 Bracket Testing

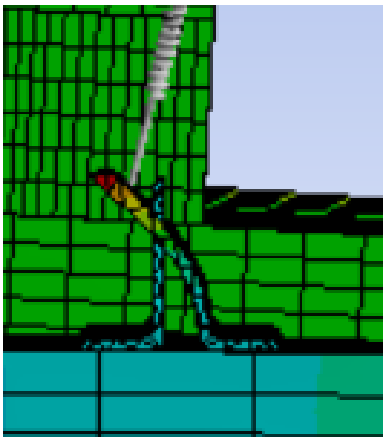

Figure 34: Deformed Turnbuckle Bracket

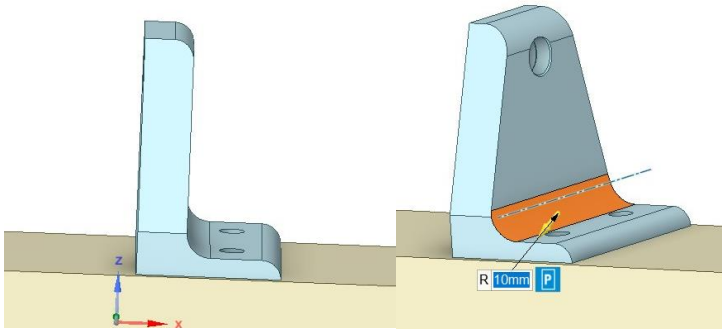

Figure 35: Upgraded Bracket Design

Next, new brackets were created to be able to not deform like figure 35. The back of the bracket was extended 10 mm and a greater fillet was added on the inner angle. The material was also upgraded to 4340 steel, which increased the stiffness of the bracket, and in turn the stiffness of

the system. Upon completion of the bracket upgrade, the center coarse adjustment stage was now stiff enough independently to continue onto the fine adjustment stage.

3.1.5 Fine Adjustment Stage

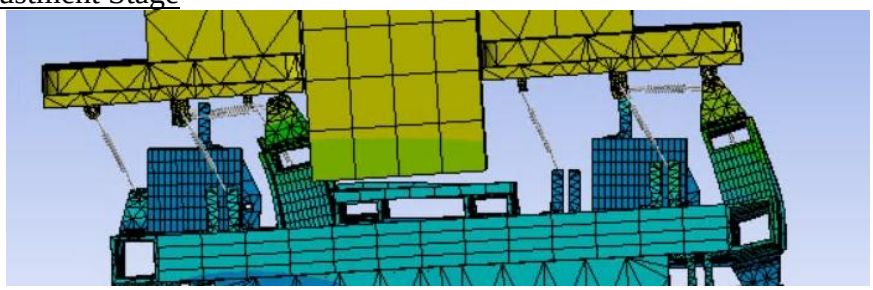

Figure 36: Fine Adjustment Stage Deformation

Figure 36 shows the deformation of the fine adjustment raft with the stiffened coarse adjustment raft. Angled stiffening pieces of 8020 were added at the corners of the raft shown in figure 37 for added stiffness.

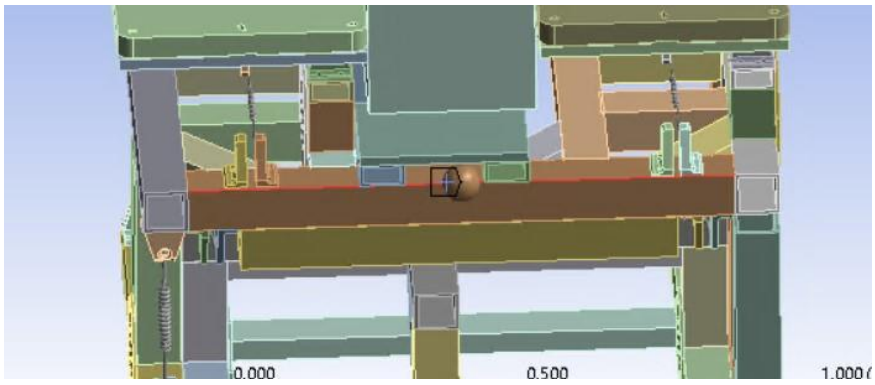

Figure 38: Added Stiffeners to Fine Adjustment Raft

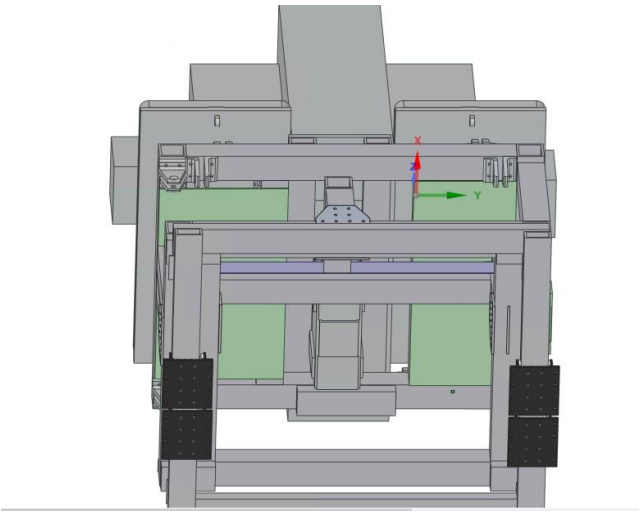

Figure 39: Steel Plating at the Bottom of Fine Adjustment Stage

After confirmation of the angled corner pieces, they were removed for 20 mm thick plates at the bottom of the raft for simplicity in fabrication. The plates functioned as the same stiffening mechanism for the upper raft.

3.1.6 Weldments

The welded tabs at the bottom of the instrumentation package also needed added stiffness, shown below in figure 40. By upgrading to a steel alloy with a great yield stress, the tab deformation was limited.

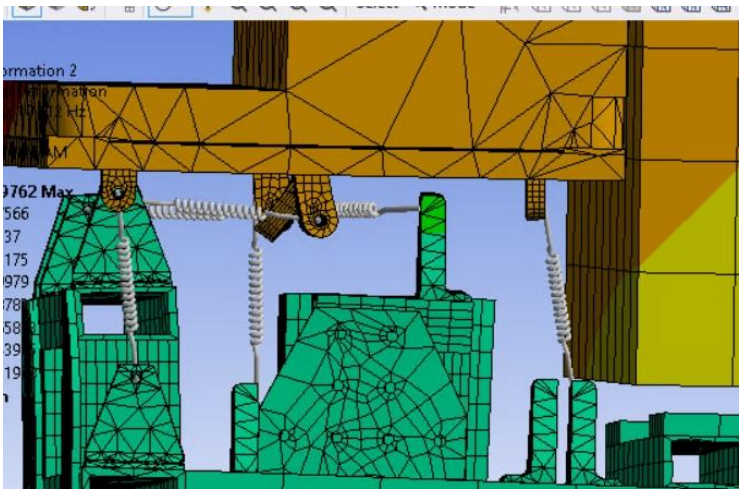

Figure 40: Deformed Tabs on Fine Adjustment Stage

3.1.7 Beam Direction Upper Raft Stiffeners

The upper raft also showed deformation on the highlighted area, moving in the beam direction.

By adding plating in figure 41, stiffness was added to the system.

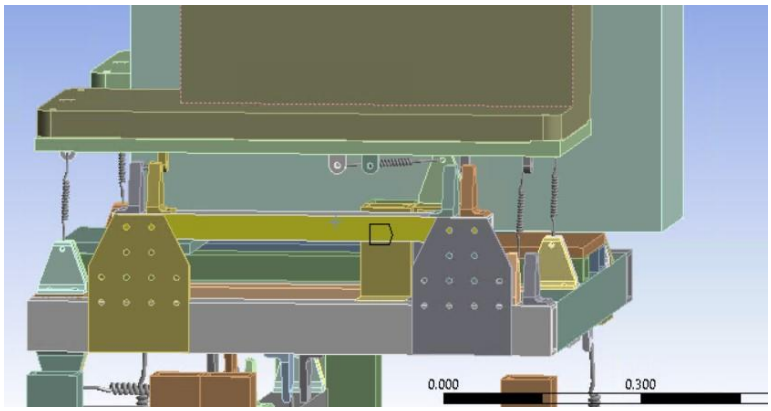

Figure 41: Portion of Upper Raft Requiring Stiffening

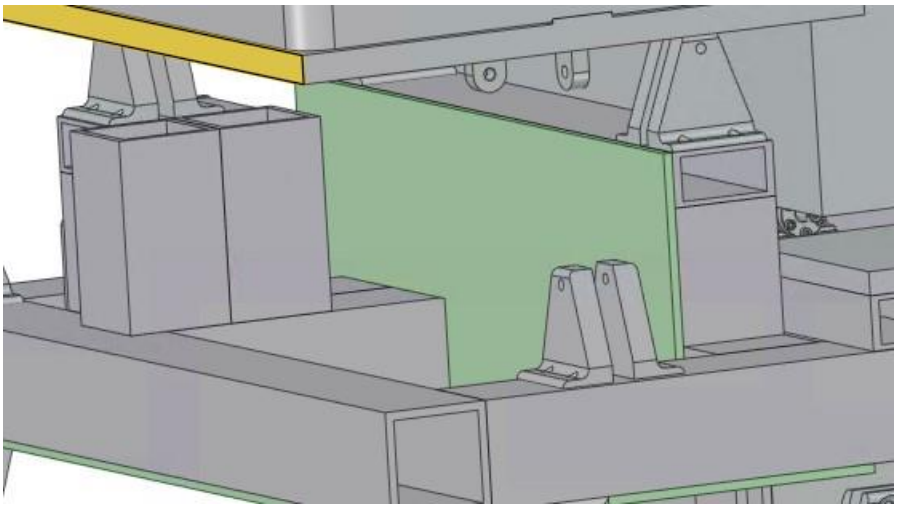

Figure 42: Added Plating to Deformed Portion of Upper Raft

This plating was replicated on both sides of the fine adjustment stage. After the addition of stiffening plates, the stand has reached frequency values comfortably within the required range, as covered in the final modal analysis results to follow.

3.2 Modal Analysis Final Results
3.2.1 Overview and Discussion of Results

Table 10: First 6 Mode Frequencies

	Mode	Frequency [Hz]
1	1.	17.559
2	2.	27.908
3	3.	32.573
4	4.	36.383
5	5.	69.73
6	6.	83.029

The first six frequency modes are above the required 15 Hz.

As shown in table 10, the unit is comfortably outside of the range of concern and exceeds the 15 Hz threshold by almost 3 Hz. It can be assumed that the unit's modes will not interact with common frequencies that will be in close relation to the stand and concerns of resonance will be minimal. Though the 15 Hz threshold is avoided, it is important to understand what is happening at each individual mode in case the unit needs to be slightly tweaked during use to accommodate for new situations or information.

The first few modes are the highest concern, as they are closest to the self-prescribed 15 Hz minimum. A description of each mode and how to properly combat whatever motion is created at each mode to make the unit stiffer to raise the potential mode values are to follow. Though it is not always best practice to just add material, through extensive research and development, the stand is a stiffness-based mechanism. If there is large deformation at a particular mode, the overall stiffness and in turn the frequency can be improved by stiffening the portion of the unit that is under high stress, like the front 8020 beam examined in mode 1.

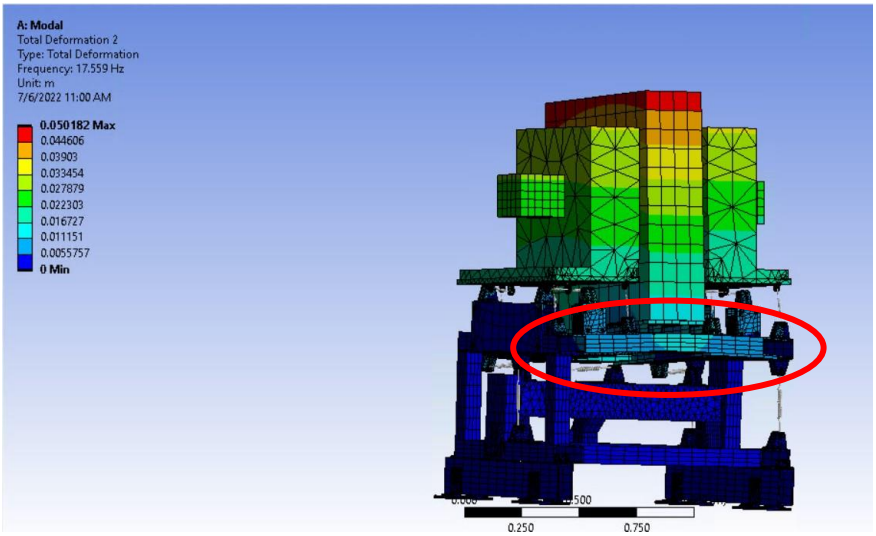

Figure 43: Mode 1

Mode 1, or the lowest frequency, exceeds the goal of 15 Hz. It is still important to understand the motion derived from mode 1 frequency to be able to either adjust the design on the in a prototype phase if more stiffness is needed, or to understand any potential problems, as unlikely as they are. The first frequency movement can be described as the front portion of the raft bending under the mass of the instrumentation, circled in red in figure 43. This is one of the easiest deformations to fix, as simply adding more 8020 channelings under the raft around the turnbuckle brackets would offer the stiffness. It is fair to assume that this deformation is not likely, as discussed earlier the perpendicular intersections of 8020 is not representative of actual strength due to internal geometry simplifications.

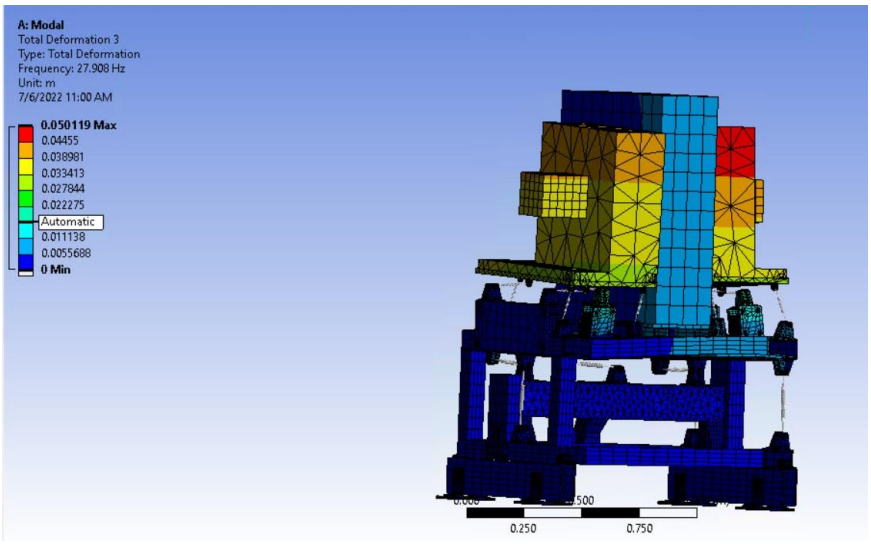

Figure 44: Mode 2

Mode 2 also greatly exceeds the goal of 15 Hz, and the movement of the raft is easy to understand and counteract if it becomes a problem when in use. The motion of mode two is also the upper raft bending, but less bending on the side-to-side spanning piece in mode 1, but more on the edges. Mode 2 deformation is likely from the edges of the "picture" frame being pulled apart from each other. This can be fixed by strengthening that connection with plating or extra fasteners.

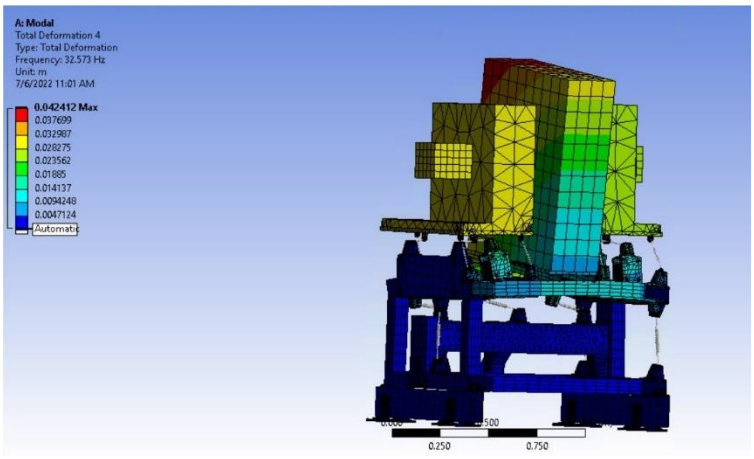

Figure 45: Mode 3

Mode 3 is similar to mode 1, with the front portion of the upper raft bending. This can be fixed by simply stiffening that portion of 8020.

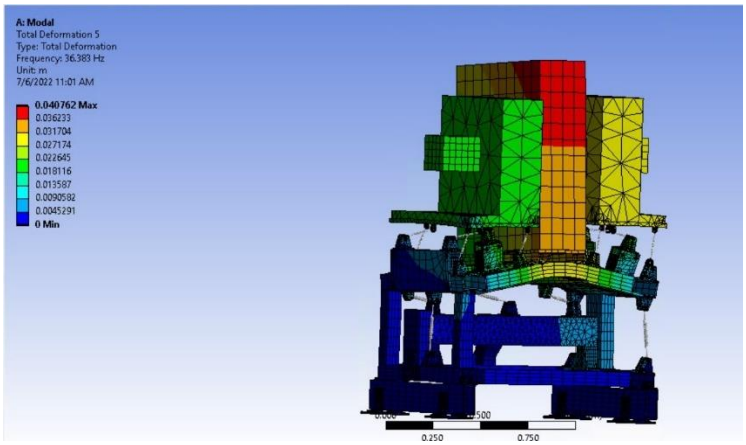

Figure 46: Mode 4

Similar to mode 3, mode 4 is a more extreme version of the bending of the front piece of 8020. The raft is bending inwards around the edges of the frame. Imagine the phenomenon of blowing a bubble. Though the frequency is high and it likely will not be a problem, to offset mode 3 motion adding stiffness to the raft is required. Additional strength can be done by adding 8020 "kickers" that run in the XY plane at a 45° angle to tie the sides into each other.

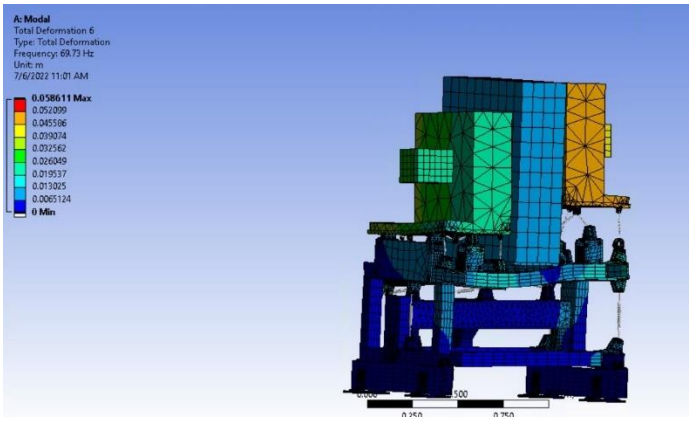

Figure 47: Mode 5

A very similar phenomenon, but mode 5deformation is caused by the left pseudo mass moving vertically. This can be offset by stiffening the center of the raft, or by upgrading the 1530 pieces of 8020 under the middle instrumentation box to a stiffer 3030 piece.

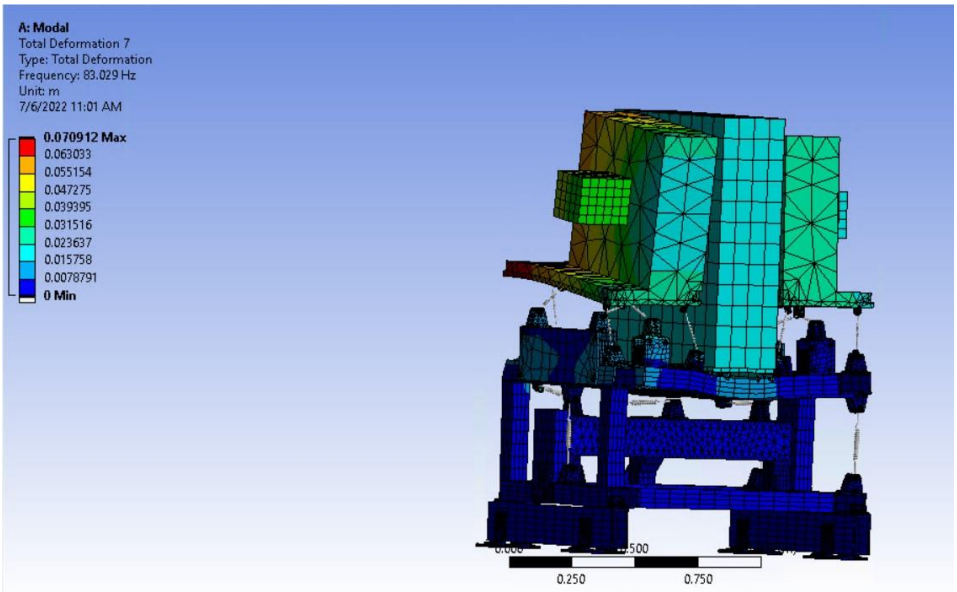

Figure 48: Mode 6

Mode 6 is like 5, but the vertical movement is derived from the right pseudo mass more than the left mass. This can be offset in the same way, or a stiffer vertical turnbuckle could be substituted to get greater resistance to the magnets moving up and down. The last two modes, modes 5 and 6, are of low concern because the frequency is so high. It is unlikely that the unit will ever cycle to the 5^{th} or 6^{th} mode and if so, it would require such a high frequency that is unlikely to happen.

Table 11: Modes with Description

Mode	Frequency	Description
1	17.559	Movement parallel to gravitational direction
2	27.908	Movement perpindicular to gravitational direction and beam line
3	32.573	Movement perpindicular to gravitational direction and beam line
4	36.383	Movement parallel to gravitational direction
5	69.73	Movement perpindicular to gravitational direction and beam line
6	83.029	Movement perpindicular to gravitational direction and beam line

3.2.2 Unique In-Situ Application Analysis

Though analysis of the unit in a nominal state with no external loading with turnbuckles at nominal lengths can paint a fairly good picture of the modal integrity of the unit, special analysis on unique situations will prove to be valuable for when the unit is in place. Special analysis was completed for "worst case loading," transportation loading and if technicians are either climbing on or leaning on the unit.

Worst case scenario loading, which is essentially when the turnbuckle lengths are adjusted in such a way to concentrate loading. A fair rule of thumb is typically understanding that the unit is at it is most unstable when all the turnbuckles are adjusted in a way that all the mass is angled down on one corner of the unit. This would mean that some vertical components are all the way out, and their opposites are all the way in. The worst overall case, from a modal standpoint, is when all the turnbuckles are in an orientation that the top raft is angled down toward the edge of the raft as shown below in figure 49.

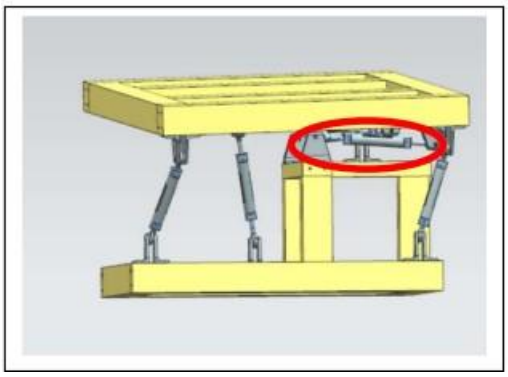

Figure 49: Worst Case loading

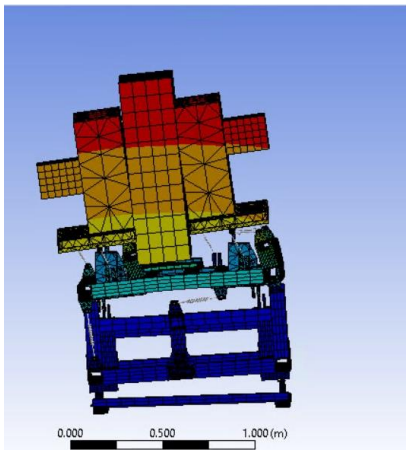

Figure 50: All Layers Converging on One Corner

The worst-case loading did make an impact on the modal stability of the unit, but not to a detrimental effect. The lowest mode value dropped approximately .4 Hz. Because the lowest mode was clear of the 15 Hz threshold, it is not of major concern. This was only one

configuration, as some of the other “worst case” loadings from a structural standpoint stiffened the unit. If the loading configuration is pulling much of the weight away from the center of gravity, then it is of concern. Some configurations pull the weight closer to the center of the unit, which improves the modal resistance to vibration. However, as the unit evolves and potentially items are added down the road, it is important to factor turnbuckle manipulation into considerations and design changes. Though not huge, it does have influence and if the unit is under extreme adjustment, like shown above, that it is not as stiff as expected.

Another unique test is confirming that the unit can withstand transport load. Extensive testing was completed by colleague Kyle Kendziora on the expected vertical loads when the unit is on the transport truck. Though his research confirmed that the loading likely will not exceed 1.5G, testing was done at 2G for extra safety. Because the unit derives its rigidity from vertical stiffness, transport loading had no effect on the modal tendencies of the unit.

The final unique testing was confirming that the unit would withstand international building code simulations but using the loading procedures only for a modal analysis. Like transportation, adding masses of workers or a technician leaning on the unit had no real impact on the modal analysis of the system.

It is to be accepted that the worst-case loading scenario can impact the overall stiffness and lower the mode one frequency slightly but not to a concerning degree, whereas transport and building code loadings had no impact on the integrity from a modal standpoint.

3.3 Future Use

3.3.1 Understanding Modal Tendencies

Though anything is technically possible as the unit approaches resonance with other moving parts in close proximity, a few patterns of motion have been recognized as the highest areas of concern. The unit can move in four main ways: in each of the three cardinal directions or a combination of the three. Some tendencies are of less concern than others, meaning that for example if the unit is moving slightly in the beam direction, we are unlikely to see that much of a performance loss. However, if the unit is moving in all three directions and moving side to side into surrounding infrastructure, then the unit is put into jeopardy. By understanding what is happening at each frequency and what paths of motion are of high concern, a better gameplan can be created for solving potential issues when in use.

3.3.2 Troubleshooting

The biggest contributor to instability is movement in the vertical direction being compounded with movement in the transverse direction. As is evident by the strut loading analysis, the vertical turnbuckles are under the greatest loading by a large margin. The greatest instability creator is when all the vertical loading causes 8020 to bend, which pulls the surrounding pieces with it and causes movement either in the beam direction or worst case in the transverse direction. Most instability at lower frequency can be traced back to deflection in one of the long 8020 beams, usually the ones spanning the transverse direction. Though unlikely, the easiest fix to instability is adding extra channeling below the deflecting piece for added bending stiffness. Stiffness could also be added by using steel plating to create a shell, essentially turning the extrusion into an I-beam.

The other big contributor is the isolated transverse brackets on the upper fine adjustment raft, highlighted on mode 2. This can be fixed in the same way, by just stiffening up that area.

3.3.3 Modal Analysis Conclusions

Through extensive analysis, it can be concluded that the 650 MHz Warm Unit Structure will meet all modal requirements while implementing design changes that will help fabrication and access. The lowest mode, approximately 17.5 Hz is far enough clear of the required 15 Hz that even slight changes will not prove to be detrimental. Various tests on unique situations were ran and it can also be concluded that the unit will be safe in transport and under accidental loading conditions, such as a technician leaning on the unit.

Chapter 4: Structural Analysis of Warm Unit Stand

4.1. Nominal Configuration Analysis

4.1.1 8020 Stress

As previously covered, the stress in 8020 material can not exceed 60% of the yield stress of the 35,000 PSI rating from 8020. This means that the unit may not exceed 144 MPa at any point.

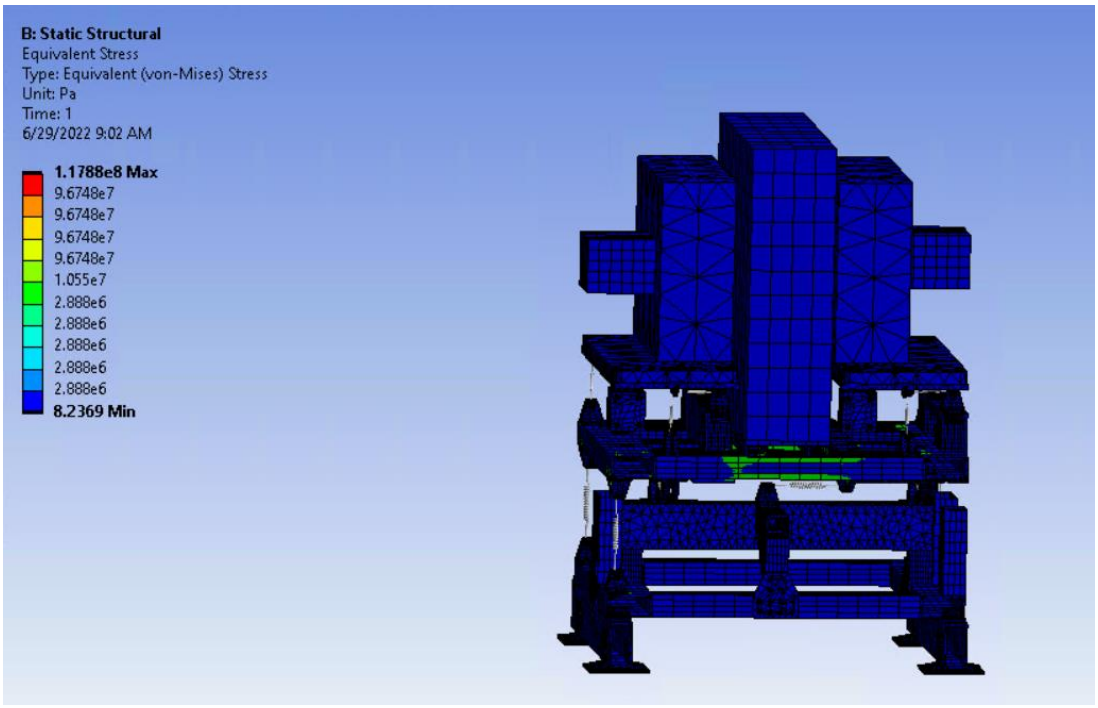

Figure 51: Equivalent Stress Distribution for Warm Unit Stand

Initial visual inspection suggests that the stress patterns are as expected. The long spanning 8020 pieces in the beam direction prove to be under the greatest stress.

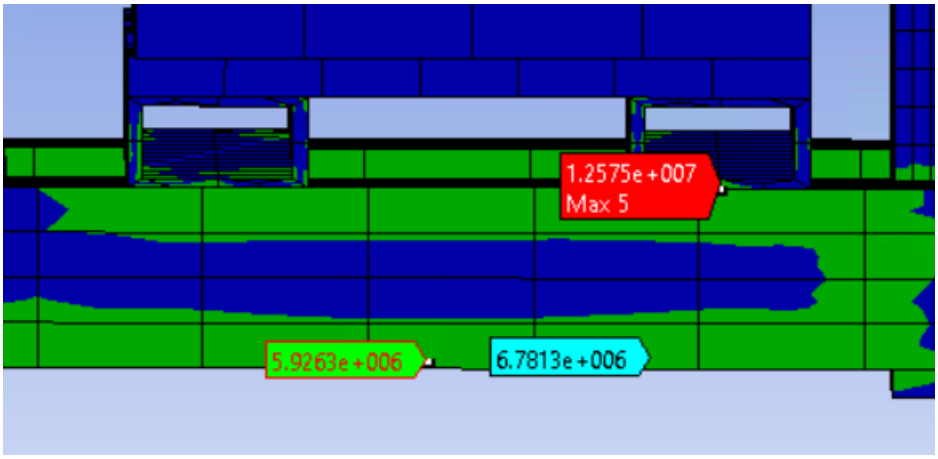

Figure 52: Maximum Stress in 8020

Figure 52 above shows that the maximum stress exerted on the 8020 frame is approximately 12.5 MPa. Since the stress is less than 15% of the raw material yield stress, it is safe to conclude that the framework is not a concern of structural failure. It is important to note that the probe states "Max 5", but that is only because the first four highest stress areas are not 8020. The first four max stresses are in the pseudo masses and are only one node, so it can be assumed that those are erroneous and a meshing issue. Other probes were placed on the beam to show that the stress is distributed throughout the 8020.

4.1.2 Turnbuckles Stress

The turnbuckles, when made of 4340 steel, can safely withstand a direct axial loading of 7000 N safely as previously mentioned. It has also been physically tested that the units can withstand close to 10 KN without significant deformation. It can be reasonably assumed that loading under 5000 N does not require greater investigation, as it is a 2.0 factor of safety on physical testing data.

The strut loads are as follows. For naming convention, the "left" side is when viewing the unit from the front, circled below. This can also be described as upstream. Outside and inside are

naming conventions for distance from the center ion pump. The “inside” is closest to ion pump, whereas “outside” is at the edge of the raft.

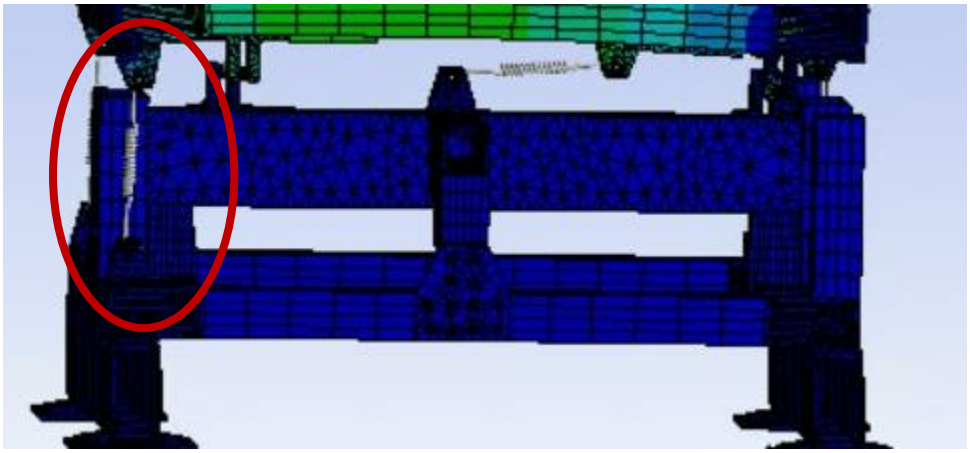

Figure 53: Strut Locations for Turnbuckle Naming

Lower raft-

Table 12: Coarse Adjust Stage Turnbuckle Stresses

Turnbuckle	Probe Reading(Newtons)
Transverse(Right)	3.9
Transverse(Left)	3.9
Beam Direction	1
Single(right) Vertical	1932.6
Front(left) Vertical	965.2
Back(left) Vertical	942.1

Testing on the large turnbuckles produced results that ***meet maximum stress requirements***. The transverse struts and the beam direction strut were under minimal loading. This is because the unit is in its nominal configuration, so the payload is not off center and causing the unit to be pulled to a side. The loading is concentrated vertically, with the load being spread out close to

evenly between all the vertical struts. The single strut side is the highest stress, as to be expected, and is still far under the 7 KN limit, not even achieving 2 KN. It is also shows that the unit distributes weight properly as the double vertical side is under the same load when combined as the single strut, +/- .1 KN.

Upper Raft-

Table 13: "Left" Side Upper Raft Stress

Turnbuckle	Probe Reading (Newtons)
Front vertical	22
Back outside vertical	149.79
Back inside vertical	299.41
Front beam direction	14.1
Back beam direction	0.4
Transverse	28.2

Table 14: "Right" Side Upper Raft Stress

Turnbuckle	Probe Reading (Newtons)
Front vertical	65.3
Back outside vertical	171.9
Back inside vertical	277.12
Front beam direction	2.5
Back beam direction	16.716
Transverse	1.79

As shown above, the loading for the upper raft is far ***below the maximum stress for the upper raft turnbuckles***. The upper raft turnbuckle is simply a half-scaled version of the coarse adjustment turnbuckles, with a tested maximum loading of 3000N, with a material failure loading of 25.2 KN. It is also important to note that both sides of the raft are relatively close on their “sister” struts. The slight differences can be a combination of either the simulation software,

or the connection tabs being placed fractions of a millimeter away from each other, however the stress pattern is similar, and the same struts carry the same percentage(approximately) of the total payload. The smaller upper struts are at no concern of failure or deformation due to their low loading. In nominal configuration it can be concluded that the turnbuckles are of no concern for permanent damage due to overloading while holding up the payload.

4.1.3 Bracket Stress

As previously stated, the maximum allowable stress for 4340 steel is 280 MPa. Testing was completed on the individual brackets for each possible loading scenario, and the stress and deformation results are as follows.

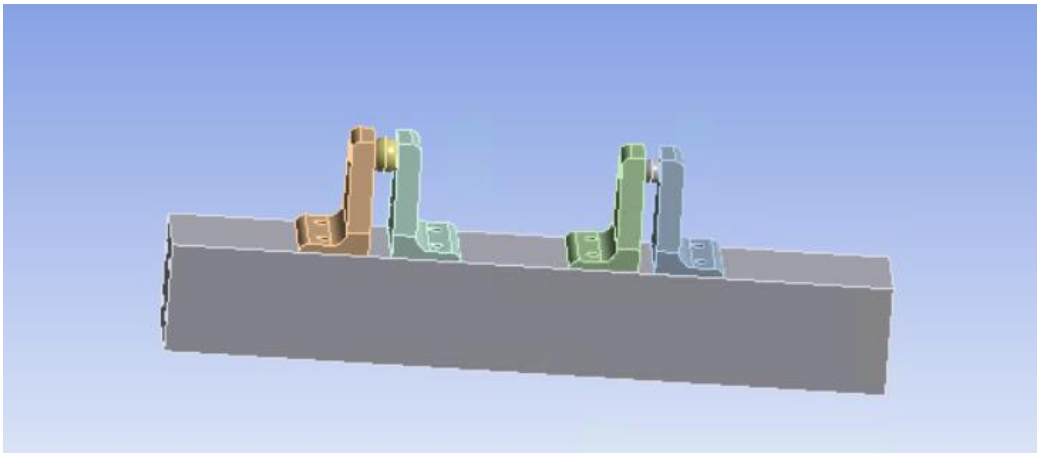

Figure 54: Bracket Force Test Mechanism

Table 15: Maximum Stress on Brackets

Bracket and direction	Deformation(Meters)	Stress(Pa)
Course Vertical	3.9 e -6	4.43 e7
Course Horizontal	0	0
Fine Vertical	2.3 e-6	8.016 e6
Fine Horizontal	1.87 e-6	6.1 e6

The bracket stress and deformation meet both requirements for safe use.

Bearing stress on the shoulder bolt was analyzed for failure as well.

- Largest force: 1902.2 N
- $F_{bearing}$ = 1902.2 cos(6.91)
- $F_{bearing}$ = 1888.3 N
- F_{shear} = 1902.2 sin(6.91)
- F_{shear} = 228.8 N
- $A_{bearing}$ = 12.7 mm * 5.35 mm = 67.9 mm^2
- A_{shear}= πtd = 106.6mm^2
- $\sigma_{bearing}=F_{bearing}/A_{bearing}$ = 13.91 MPa
- $\tau=F_{shear}/A_{shear}$ =2.14 MPa

- Maximum allowable bearing stress(per McMasterCarr): 579 MPa
- Maximum shear: 347.4 MPa

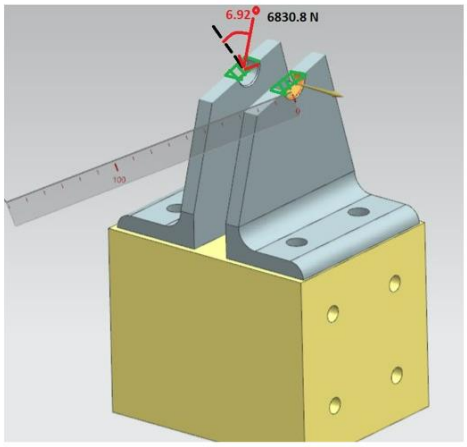

Figure 55: Vertical Bearing Stress

- Maximum Horizontal Force: 111.1 N
- $\sigma_{bearing}$=1.63MPa
- $\tau=_{Fshear/Ashear}$ =.08 MPa

•Maximum allowable bearing stress(per McMasterCarr): 579 MPa
•Maximum shear: 347.4 MPa

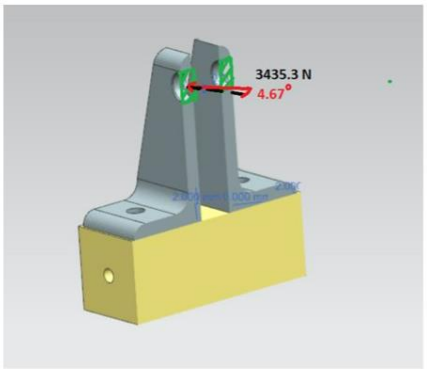

Figure 56: Horizontal Bearing Stress

As shown in the figures 55 and 56 above, the stresses for the maximum force on the brackets were calculated. The coarse stage vertical had the greatest stress, as to be expected, but it should easily be able to withstand the loading. The deformation in all levels was negligible, so it can be assumed that the brackets will easily be able to support the weight of the system if using mild steel.

4.2 Nominal Configuration Conclusions

4.2.1 Code compliance

Upon analyzing the three primary areas of concern, the bracketing, turnbuckles and 8020 framework, it can be concluded that all code and proper engineering techniques were followed and met for the nominal configuration. The greatest stress on the 8020 material is far below the maximum allowable and can easily withstand 2-3x the expected loading without concern of fatigue or failure. The turnbuckles and the brackets are at a similar level of compliance to maximum loading and deformation practices, with both values a mere fraction of the maximum allowable stress. It is critical that the different components are so far away from the maximum range, as other parts of the project continue to evolve. The unit needs to be able to withstand a possible increase in payload or any other obstacle yet to come.

4.2.2 Troubleshooting

Though not a concern, it is important to have best practice protocols in place if the unit begins to show early signs of fatigue or deformation. Through extensive testing, it can be concluded that the unit will show fatigue in three ways; the long spanning 8020 pieces bending, the brackets bending inwards, or the turnbuckles bending. The 8020 is the simplest to fix, as simply adding more channel to the concern areas, or steel plating would be a simple fix that could be done by one technician. Table 16 shows the most effective way to combat the most common areas of deformation.

Table 16: Potential Deformation Solutions

Area of Deformation	Potential solution
Large 8020 vertical deflection, or bending	Steel plating, or thicker 8020
Bracket bending(inward)	Thicker bracket, or upgrade to a stronger steel alloy
Turnbuckle bending	Stronger steel alloy

Figure 57: Bracket Deformation

As shown in figure 57, unit axial vertical stress, the unit can begin to slightly deform. By upgrading the steel alloy, that concern can be mitigated.

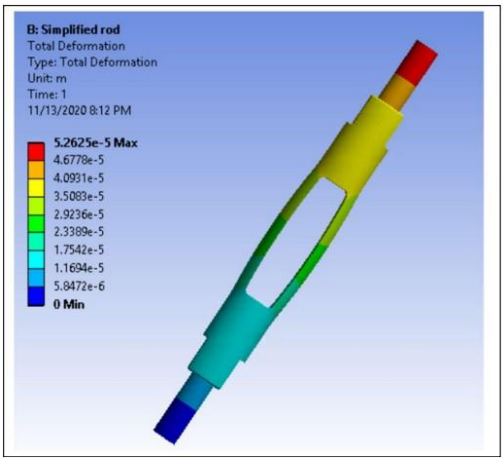

*Figure 58: Rod Bending *Photo Courtesy of Chris Becker*

It should be noted that none of these should need to be implemented, as everything is far below maximum allowable ranges, though it is good practice to have protocol.

4.2.3 Stiffening for Potential Added Instrumentation

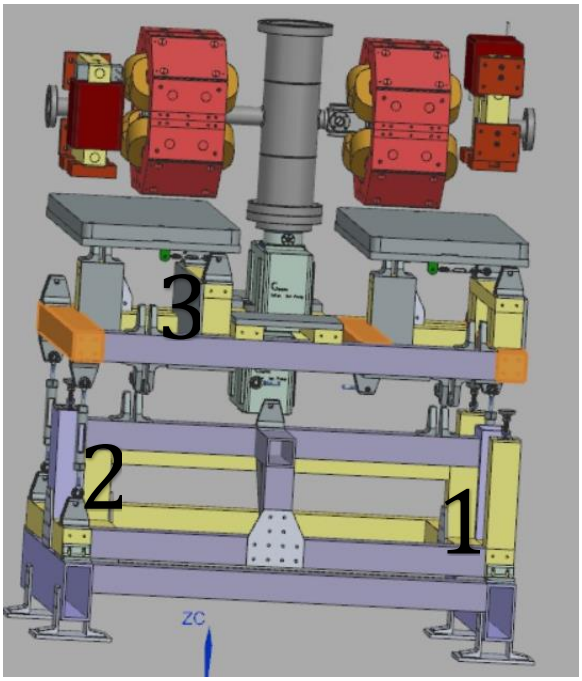

Figure 59: Stiffening Locations for Added Instrumentation

Though analysis confirms that it will not be required for current payload expectations, stiffening in each direction can be described in figure 59 if other design groups require significant design change. Stiffening in the transverse direction, or “in and out” of the page, will be done by stiffening the connection marked one. It is likely that the inside yellow piece will pull away from the outside purple one as the first major deformation in the transverse direction. Similarly, in the beam direction, stiffening the upper raft beam length turnbuckle platform would be the simplest and most effective fix to needing more beam length stiffness. Finally, vertical stiffness can only really be controlled by the strength of the turnbuckle or the screw jacks. This can be done by upgrading the material on the turnbuckles.

4.3 Worst Case Scenario Analysis
4.3.1 8020 Stress

The stipulations laid out for the nominal configuration will be the same for the worst-case scenario loading. The 8020 cannot exceed 84 MPa at any portion that is constructed of 8020 aluminum extrusion. The same exact simulation was run and the results, for 8020, were close to nominal configuration. The greatest stress, shown below, was approximately 14.4 MPa. Though slightly larger than the nominal configuration, it is of no big concern as it still is below the stress range of concern. Deformation was also almost non-existent, only moving fractions of a millimeter.

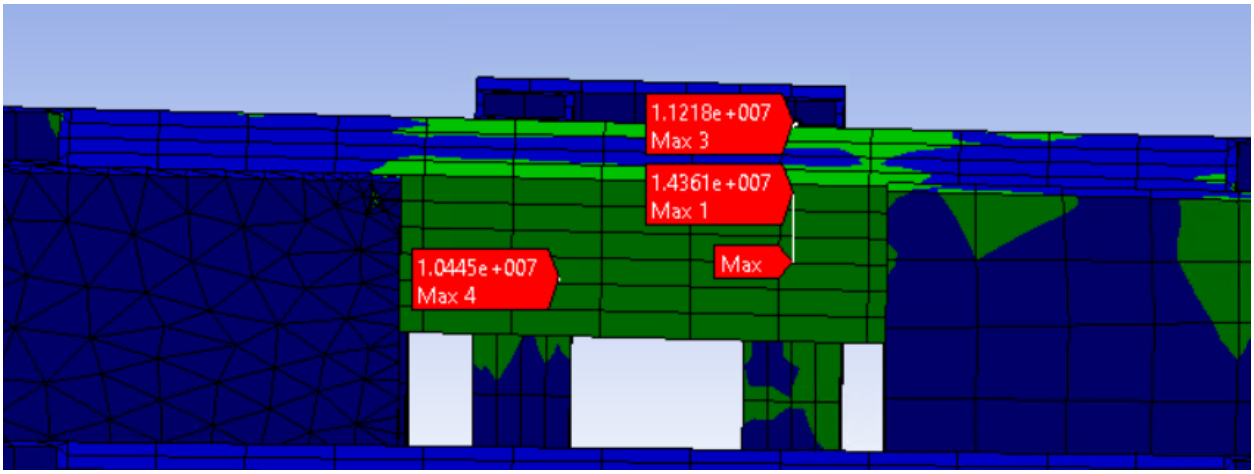

Figure 60: Maximum Stress on 8020

4.3.2 Turnbuckle Stress

The same testing on the turnbuckles were to be completed as was done in nominal configuration. The same maximum loads still apply, and the simulation was done the same exact way, with the only change being the struts moved slightly to accommodate the "worst case" configuration.

Table 17: Coarse Adjustment Turnbuckles

Turnbuckle	Probe Reading(Newtons)
Transverse(right)	25.5
Transverse(left)	111.1
Beam Direction	64.268
Single(right) Vertical	1902.1
Front Vertical on left	907.1
Back Vertical on left	1049.6

Shown above, the maximum force applied on the turnbuckles are below the 7 KN maximum limit. The weight distribution changed slightly, to favor the backside, but not to a level of concern. This should be obvious, as the weight is now slanted in the direction of the back vertical strut. The non-vertical struts are under greater load now that the masses are off center, but the loading is still far below any level of concern.

Table 18: Left Upper Raft Turnbuckles

Turnbuckle	Probe Reading (Newtons)
Front vertical	12.7
Back outside vertical	39.2
Back inside vertical	198.8
Front beam direction	3.5
Back beam direction	9.7
Transverse	7.2

Table 19: Right Upper Raft Turnbuckles

Turnbuckle	Probe Reading (Newtons)
Front vertical	76.56
Back outside vertical	159.4
Back inside vertical	252.5
Front beam direction	0.5
Back beam direction	21.9
Transverse	0.01

The left and right upper raft turnbuckles are both below the maximum allowable force.

Like the larger coarse adjustment turnbuckles, the worst-case scenario loading changed the stress distribution slightly, but not to a level of concern for the overall integrity of the unit. As is evident when coMParing to nominal loading, the vertical stresses are a tad more concentrated, on the inside vertical strut on the right side and the inside vertical strut on the left side, but the overall magnitude of the stresses is of no concern whatsoever.

4.3.3 Bracket Stress

Table 20: Bracket Deformation and Stress

Bracket and direction	Deformation(Meters)	Stress(Pa)
Course Vertical	3.9 e-6	4.36 e7
Course Horizontal	1.5 e-6	3.98 e6
Fine Vertical	1.9 e-6	6.78 e6
Fine Horizontal	1.45 e-7	6.11 e6

The bracket is far below the maximum allowable stress and deformation.

In the same exact method to the nominal testing, the bracket stress was calculated using the strut values from the worst-case scenario loading. Like nominal, the loads will be completely clear of the concern level of stress, with the maximum stress being approximately 43 MPa. It is important to note that the horizontal strength is not as great as the vertical, so if the unit continues to have

more horizontal loading due to added pieces in the future, bracket adjustments or material change may be necessary.

4.3.4 Code compliance

The worst-case scenario loading stress and force values were far within an acceptable range. Similarly to nominal configuration, none of the maximum values approach the upper range of the allowable maximum value. This is preferred, as the unit and payload can continue to evolve. The maximum allowable stress for the 8020 was 84 MPa, where the maximum stress in use did not exceed 15 MPa. Physical testing on a turnbuckle prototype was completed by Kyle Kedriozia that concluded that the unit could comfortably withstand 10 KN of loading in tension and 9.8 KN of loading in compression without any noticeable deformation or fatigue.

Figure 61: Instron Tension and Compression Testing

Similarly, the turnbuckles did not exceed a 2 KN force, far below the maximum of 7 KN. Finally, the brackets showed minimal deformation and the stress was far below the allowable maximum, with the maximum stress being approximately 43 MPa, far below the 120 MPa maximum prescribed for a 60% value of mild streel yield strength.

4.3.5 Troubleshooting/ Future Stiffening

Though the weight was slightly redistributed, the overall behavior of the system did not change dramatically in the worst-case loading. Fixing the unit for fatigue parts would follow the same method as nominal configuration. Though it should be noted that it is likely that when not in nominal configuration a greater emphasis will be placed on the non-vertical supports.

4.4 International Building Code

4.4.1 Analysis Parameters

To ensure that the unit is safe for continued use, international building code (IBC) was followed. Due to various circumstances, the unit being inside and not exposed to seismic loading for example, simplified the IBC analysis. For this unit, the dead load, incidental live load, fluid loads and interface loads are the only areas of concern.

The dead load, just the payload with a 10% FDR level buffer, can be calculated as follows:

- Single quad package (1): 350kg (+10%) = 385kg
- Single corrector package (2): 65kg (+10%) = 71.5kg
- Instrumentation package (3): 100kg (+10%) = 110kg

The fluid load can be estimated at 2 kg, whereas the interface loads are minimal and can be assumed to be negligible. Interface loading for this unit is just the weight of the hoses at fluid connection points, so assuming negligible is acceptable.

The live load is strictly horizontal. A reasonable assumption that the unit will not be able to be climbed allows for a 980 N handrail representative horizontal force to be the only live load necessary for loading. The handrail load was moved to different portions of the stand, but the worst loading placement was on the upper raft, shown below.

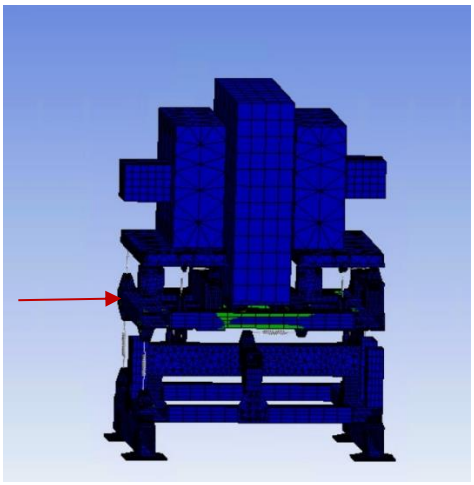

Figure 62: Handrail loading

4.4.2 International Building Code Analysis

Table 21: IBC Loading

Turnbuckle	Probe Reading(Newtons)
Lower Raft:	
Transverse(Right)	51.1
Transverse(Left)	227.7
Beam Direction	165.1
Single(right) Vertical	953.6
Front(left) Vertical	1112.8
Back(left) Vertical	2388
"Left" Upper Raft:	
Front Vertical	1240.6
Back Outside Vertical	467.3
Back Inside Vertical	1540.2
Front Beam Direction	27.2
Back Beam Direction	13.6
Transverse	196.4
"Right" Upper Raft:	
Front Vertical	1232.9
Back Outside Vertical	465.3
Back Inside Vertical	1545.3
Front Beam Direction	68.97
Back Beam Direction	58.8
Transverse	31.6

All turnbuckles are far below maximum allowable force.

Though the loading on turnbuckles will be greater under IBC loading conditions, each turnbuckle is still far under maximum allowable loading, meaning that IBC is met and satisfied

4.5 Miscellaneous Testing

4.5.1 Transport loading

When the unit is in transport, it will experience a greater vertical force than when it is in use. Work was done by Kyle Kendziora to determine the directional forces on a unit loaded on a transport truck. The vertical force was the only directional force that changed dramatically likely due to the truck hitting bumps on the road. It was determined that the unit when transported would not exceed 2G or double the vertical force of typical use. It is also determined that the unit would be transported in nominal configuration, as adjustments cannot take place until the unit is observed in relation to surrounding infrastructure.

Transportation loading analysis is simple, by simple doubling the forces, it can replicate the extremes of transportation displacement in the vertical direction. The maximum forces are the same as the other configurations.

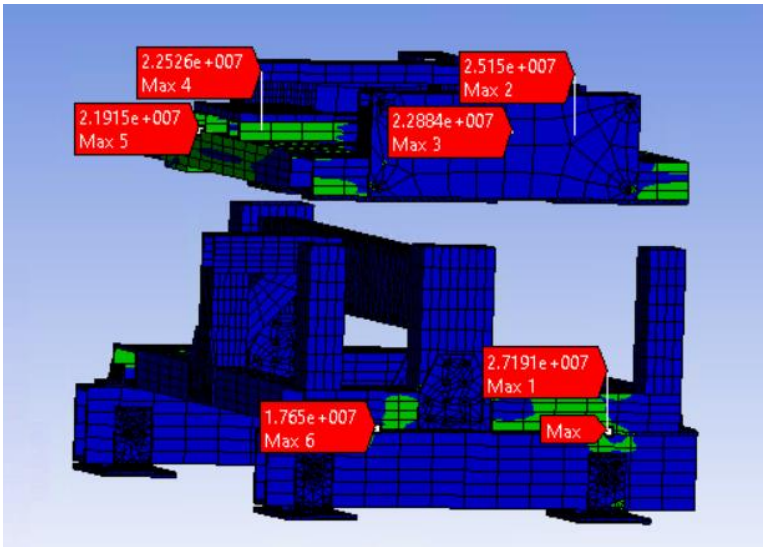

Figure 63: 8020 Maximum Stresses

As shown above, the maximum stress during transportation loading is approximately 27.2 MPa, well below the maximum allowable stress.

Table 22: Coarse Adjustment Stage Turnbuckles

Turnbuckle	Probe Reading(Newtons)
Transverse(right)	7.89
Transverse(left)	7.89
Beam Direction	0
Single(right) Vertical	3865.3
Front Vertical on left	1930.5
Back Vertical on left	1884.2

Table 23: Upper Raft Left Side Turnbuckles

Turnbuckle	Probe Reading (Newtons)
Front vertical	44
Back outside vertical	299.5
Back inside vertical	598.8
Front beam direction	28.1
Back beam direction	0.7
Transverse	56.5

Table 24: Upper Raft Right Side Turnbuckles

Turnbuckle	Probe Reading (Newtons)
Front vertical	130.7
Back outside vertical	343.7
Back inside vertical	554.2
Front beam direction	5.1
Back beam direction	33.4
Transverse	3.5

All levels of turnbuckles meet maximum force requirements.

Shown above is the force applied on all eighteen turnbuckles. Using the same maximum allowable force from previous work, it can be determined that the transport load, though a greater stress on the turnbuckles, will not exceed the limit, or come close.

Finally, the brackets will be under a greater stress using transport simulation loading. For simplicity, just the maximum vertical and horizontal loads were placed on the brackets, as it would be redundant to evaluate all.

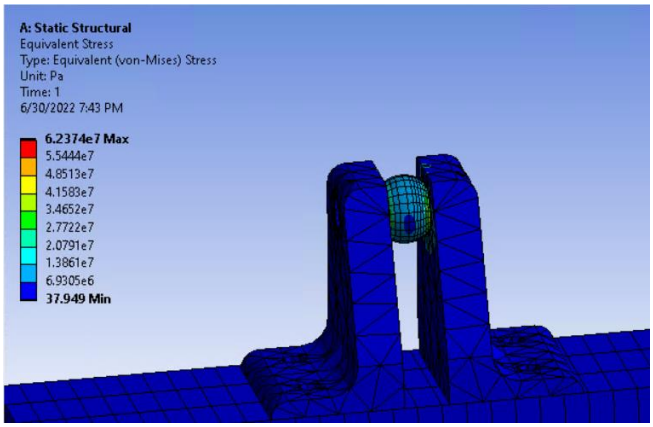

Figure 64: Vertical Loading Stress

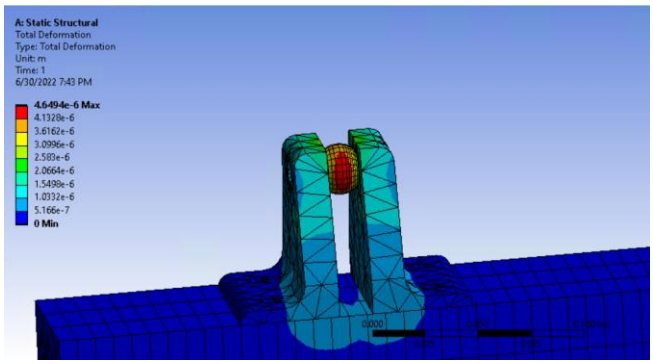

Figure 65: Vertical Loading Deformation

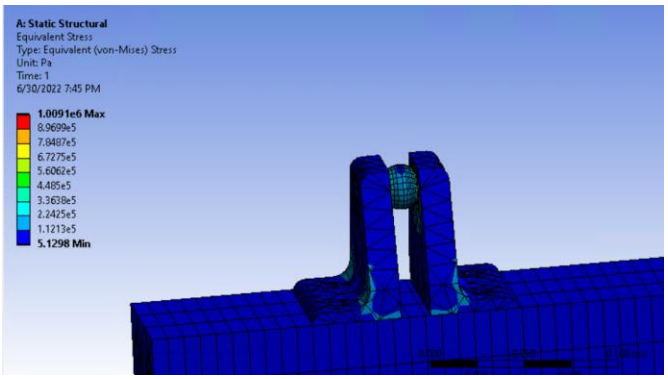

Figure 66: Horizontal Loading Stress

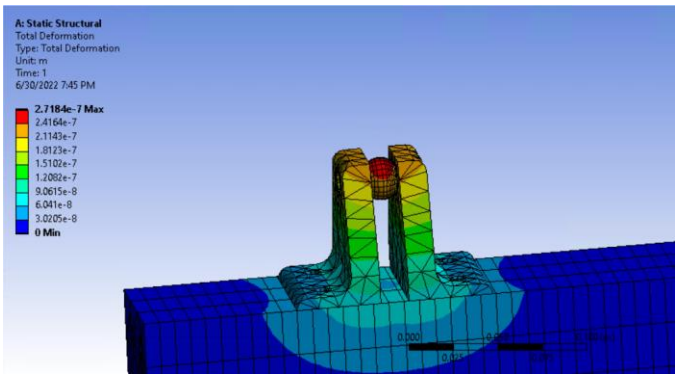

Figure 67: Horizontal Loading Deformation

The maximum stress in each configuration is far below the maximum allowable range. The vertical loading has the largest stress, at approximately 63 MPa, far below the limit of 4340 steel.

4.6 Structural Analysis Conclusions

It can be concluded that the unit will be able to withstand the total payload without concern throughout the entire lifespan of the project. It can also be concluded that the unit can withstand a payload increase without any concern for the integrity of the unit.

In both the nominal configuration, and the worst-case scenario loading, the unit is far below the maximum material stress for all the different components. It is also able to be transported and withstand the added loading from the transportation truck. The only thing to keep in mind is the unit cannot travel in a “worst case” loading configuration. Though it would make no physical sense to do so, it is important to keep the unit as close to nominal configuration

as possible for transportation. The Warm Unit stand also meets all international building code requirements.

Chapter 5: Summary and Conclusion

5.1 Analysis Summary

Throughout the lifespan of the Warm Unit stand operation, designs implemented will help technicians with access to instrumentation, allow for separate alignment based on real-world scenarios, and meet load and vibration requirements. The first critical design requirement of the Warm Unit stands is to satisfy the minimum natural frequencies. Table 25 indicates the multiple modes present when all design implementations are included in the model.

Table 25: Modal Analysis Results

Modal Analysis Results Summary			
Mode	Frequency(Hz)	Minimum Allowable(Hz)	Satisfied(Y/N)
1	17.559	15	Y
2	27.908	15	Y
3	32.573	15	Y
4	36.383	15	Y
5	69.73	15	Y
6	83.029	15	Y

The minimum frequency mode exceeds the minimum requirement by 75% and is a 16% improvement over the increased criterion of 15 Hz. Due to these features, the structure should have limited transmission of vibrations from adjacent components through the concrete pad.

In terms of force loading, the dimensions and materials of the components in the Warm Unit stand meet the stress and loading limits indicated in Table 26. The material stresses of aluminum and steel are orders of magnitude less than the yield requirements. Furthermore, the loads expected in the struts from the pseudo-masses and wheel base manage the distribution into 3 main vertical struts. The experimental testing confirm loading that was more than 4.5 times the expected compression force in the strut.

Table 26: Structural Analysis Nominal Configuration Results Summary

Nominal Configuration Results Summary			
	Force or Stress Reading	Maximum Allowable Force or Stress	Satisfied(Y/N)
8020 Maximum Stress	12.6 MPA	241 MPA	Y
Bracket Maximum Stress	44.3 MPA	240 MPA	Y
Turnbuckle	Probe Reading(Newtons)		
Lower Raft:			
Transverse(Right)	3.9	23614 N	Y
Transverse(Left)	3.9	23615 N	Y
Beam Direction	1.2	23616 N	Y
Single(right) Vertical	1932.6	23617 N	Y
Front(left) Vertical	965.2	23618 N	Y
Back(left) Vertical	942.1	23619 N	Y
"Left" Upper Raft:			
Front Vertical	22.3	25199 N	Y
Back Outside Vertical	149.7	25200 N	Y
Back Inside Vertical	299.4	25201 N	Y
Front Beam Direction	14.1	25202 N	Y
Back Beam Direction	0.4	25203 N	Y
Transverse	28.2	25204 N	Y
"Right" Upper Raft:		25206 N	
Front Vertical	65.3	25207 N	Y
Back Outside Vertical	171.9	25208 N	Y
Back Inside Vertical	277.1	25209 N	Y
Front Beam Direction	2.5	25210 N	Y
Back Beam Direction	16.7	25211 N	Y
Transverse	1.8	25212 N	Y

Given the adjustability of the Warm Unit stand and its requirement for transportation from assembly to installation, the two additional evaluation criteria were considered: twice gravitational load and off-nominal structure. Both elements in combination do increase the forces and stresses as indicated in Table 27. Conveniently, the robust design is able to withstand the increases without concern for displacement or structural failure.

Table 27: Worst Case Loading Results Summary

Worst Case Loading Results Summary			
	Force or Stress Reading	Maximum Allowable Force or Stress	Satisfied(Y/N)
8020 Maximum Stress	14.4 MPA	241 MPA	Y
Bracket Maximum Stress	43.6 MPA	240 MPA	Y
Turnbuckle	Probe Reading(Newtons)		
Lower Raft:			
Transverse(Right)	25.5	23614 N	Y
Transverse(Left)	111.1	23615 N	Y
Beam Direction	64.2	23616 N	Y
Single(right) Vertical	1902.2	23617 N	Y
Front(left) Vertical	907.1	23618 N	Y
Back(left) Vertical	1049.6	23619 N	Y
"Left" Upper Raft:			
Front Vertical	12.7	25199 N	Y
Back Outside Vertical	39.2	25200 N	Y
Back Inside Vertical	198.8	25201 N	Y
Front Beam Direction	3.5	25202 N	Y
Back Beam Direction	9.7	25203 N	Y
Transverse	7.2	25204 N	Y
"Right" Upper Raft:		25206 N	
Front Vertical	78.6	25207 N	Y
Back Outside Vertical	159.4	25208 N	Y
Back Inside Vertical	252.5	25209 N	Y
Front Beam Direction	0.5	25210 N	Y
Back Beam Direction	21.9	25211 N	Y
Transverse	0.01	25212 N	Y

5.2 Conclusion

The complete model and preliminary analysis report were included as part of the PIP-II Final Design Review on July 20, 2022. The review panel of peer engineers provided preliminary approval of the design results with only minor elements requiring further verification in a response. A final peer review on engineering documents prepared for Fermilab are the final step before pre-production prototyping is to begin.

Given the acceptance of design improvement and analysis, risks of future performance will be mitigated through fabrication of a pre-production prototype. The layered elements of the 8020 materials will be purchased from a vendor allowing the team to practice procurement and quality assurance activities. Upon receipt of each component, the dimensional check of the vendor-produced assembly will be required. A team of Fermilab technicians and NIU students

will then assemble the different layers of the Warm Unit stand. Future experimental testing will include:

- Translation of struts through full extension and retraction individually and in combination
- Confirmation of the position and rotation limits of upper magnet support and the full raft
- Ability to maintain three-point contact with the insertion rails
- Structural tests that will exceed expected loads by at 50%
- Vibration tests with impact hammers to quantify the resonance frequencies of the structure.

Reporting from the experiments will be compared to the trends observed from model analysis reported here. If in-situ design improvements are necessary, the important control features highlighted in this thesis will help with future improvements.

References

8020. (2022). *8236-Black Angle Profile*. Retrieved from https://8020.net/8236-black.html

8020, I. (2022). *3030 Extrusion Geometry* . Retrieved from https://8020.net/30-3030.html

ANSYS, I. (2022). *ANSYS Meshing Lesson 4* . Retrieved from https://courses.ansys.com/index.php/courses/transonic-flow-over-a-wing-3d/lessons/meshing-lesson-4/topic/sizing-the-mesh/

ANSYS, Inc. . (R2020). *Ansys® Workbench* .

Baffes, C. (n.d.). *ED0002931*. Batavia: FERMILAB.

Becker, C. (2021). *WARM UNIT ROD MOVEMENT STAND FOR PROTON IMPROVEMENT PROJECT II.* Dekalb: Northern Illinois University .

FERMILAB. (n.d.). *FESHM Chapter 5100- Structural Safety* . Batavia.

Lebedev, V. (2015). *The PIP-II Reference Design Report* . Batavia : Fermilab.